

TIE2-Expressing Monocytes as a Diagnostic Marker for Hepatocellular Carcinoma Correlates With Angiogenesis

Tokuhiro Matsubara,¹ Tatsuya Kanto,¹ Shoko Kuroda,¹ Sachiyo Yoshio,¹ Koyo Higashitani,¹ Naruyasu Kakita,¹ Masanori Miyazaki,¹ Mitsuru Sakakibara,² Naoki Hiramatsu,¹ Akinori Kasahara,¹ Yoshito Tomimaru,³ Akira Tomokuni,³ Hiroaki Nagano,³ Norio Hayashi,⁴ and Tetsuo Takehara¹

Angiogenesis is a critical step in the development and progression of hepatocellular carcinoma (HCC). Myeloid lineage cells, such as macrophages and monocytes, have been reported to regulate angiogenesis in mouse tumor models. TIE2, a receptor of angiopoietins, conveys pro-angiogenic signals and identifies a monocyte/macrophage subset with pro-angiogenic activity. Here, we analyzed the occurrence and kinetics of TIE2-expressing monocytes/macrophages (TEMs) in HCC patients. This study enrolled 168 HCV-infected patients including 89 with HCC. We examined the frequency of TEMs, as defined as CD14+CD16+TIE2+ cells, in the peripheral blood and liver. The localization of TEMs in the liver was determined by immunofluorescence staining. Micro-vessel density in the liver was measured by counting CD34+ vascular structures. We found that the frequency of circulating TEMs was significantly higher in HCC than non-HCC patients, while being higher in the liver than in the blood. In patients who underwent local radio-ablation or resection of HCC, the frequency of TEMs dynamically changed in the blood in parallel with HCC recurrence. Most TEMs were identified in the perivascular areas of tumor tissue. A significant positive correlation was observed between micro-vessel density in HCC and frequency of TEMs in the blood or tumors, suggesting that TEMs are involved in HCC angiogenesis. Receiver operating characteristic analyses revealed the superiority of TEM frequency to AFP, PIVKA-II and ANG-2 serum levels as diagnostic marker for HCC. Conclusion: TEMs increase in patients with HCC and their frequency changes with the therapeutic response or recurrence. We thus suggest that TEM frequency can be used as a diagnostic marker for HCC, potentially reflecting angiogenesis in the liver. (HEPATOLOGY 2013;57:1416-1425)

See Editorial on Page 1294

Hepatocellular carcinoma (HCC) is one of the most prevalent malignancies and the third leading cause of cancer-related deaths worldwide.¹ Clinically, HCC frequently develops from liver cirrhosis, with most etiologies involving hepatitis B and C virus (HBV and HCV) infection.^{2,3} Since the major-

ity of HCCs are characterized by a florid intra-tumoral vasculature, angiogenesis is deemed to be a critical step in the development and progression of HCC.⁴ Some clinical studies have demonstrated that the degree of vascularity in HCC tissues correlates with the severity of the disease condition,⁵ suggesting that prevention of this process could have beneficial impact on patient prognosis. However, the precise mechanisms of HCC-related angiogenesis in the liver remain obscure.

Abbreviations: AFP, α -fetoprotein; ANG, angiopoietin; BCLC, Barcelona-Clinic Liver Cancer; CH, chronic hepatitis; CT, computed tomography; HBV, hepatitis B virus; HCC, hepatocellular carcinoma; HCV, hepatitis C virus; LC, liver cirrhosis; MIF, macrophage migratory inhibitory factor; MRI, magnetic resonance imaging; PBMC, peripheral blood mononuclear cells; PIVKA-II, protein induced by vitamin K absence or antagonist II; ROC, receiver operating characteristic; sVEGFR-1, soluble vascular endothelial growth factor receptor-1; TEMs, TIE2-expressing monocytes; VEGF, vascular endothelial growth factor.

From the ¹Department of Gastroenterology and Hepatology, Osaka University Graduate School of Medicine, Osaka, Japan; ²Department of Osaka Medical Center for Cancer and Cardiovascular Diseases, Osaka, Japan; ³Department of Surgery, Osaka University Graduate School of Medicine, Osaka, Japan; and ⁴Kansai Rosai Hospital, Hyogo, Japan.

Received February 16, 2012; accepted June 13, 2012.

Supported in part by a Grant-In-Aid for Scientific Research from the Ministry of Education, Culture, Sports, Science, and Technology, Japan and a Grant-In-Aid from the Ministry of Health, Labor, and Welfare of Japan.

In general, two types of components are cooperatively involved in the progression of angiogenesis: humoral angiogenesis factors and vascular progenitor cells.⁴ Many studies have reported that angiogenesis factors produced from HCC drive tumor vascularization, which supports the development and progression of liver cancer, including invasion and metastasis.⁶ Among such factors, serum levels of angiopoietin-2 (ANG-2), macrophage migration inhibitory factor (MIF), vascular endothelial cell growth factor (VEGF), and soluble vascular endothelial cell growth factor receptor-1 (sVEGFR-1) have been reported to be higher in HCC patients than non-HCC subjects and to correlate with poorer prognosis or survival.⁷⁻¹¹ However, such angiogenesis molecules have failed to show any advantage over other clinically available markers for HCC diagnosis.¹²

Hematopoietic lineage cells, including hematopoietic progenitors and myeloid lineage cells, have been implicated in the promotion of tumor angiogenesis.⁴ Tyrosine kinase with Ig and EGF homology domains 2 (TIE2) is a receptor of angiopoietins (ANGs); it is primarily expressed on endothelial cells and is capable of binding to all the known ANGs (ANG-1, ANG-2 and ANG-3/ANG-4). TIE2-expressing monocytes (TEMs) are a recently described subpopulation of peripheral and tumor-infiltrating myeloid cells presumed to be equipped with profound pro-angiogenic activity; these cells are found both in mice and humans.¹³⁻¹⁵

Among human cancers, TEMs have been reported in tumors of the kidney, colon, pancreas and lung, as well as in soft tissue sarcomas,¹⁵ where angiogenesis is known to be important for tumor progression. However, it is not known whether TEMs are present in HCC, and their significance for the pathophysiology of the disease remains to be investigated.

In this study, we analyzed TEMs in HCC patients by investigating their frequency, localization and correlation with microvessel density and other clinical parameters in HCC patients. Our findings suggest that TEMs could serve as a diagnostic marker of HCC.

Materials and Methods

Subjects

Among chronically HCV-infected patients who had been followed at Osaka University Hospital, 168 patients

Table 1. Clinical Background of Subjects

Clinicopathologic Characteristics	CH	LC	HCC
Gender: male/female	21/28	13/17	63/26
Age: mean \pm SD	63.4 \pm 7.8	67.5 \pm 8.8	70.0 \pm 7.0
Alanine aminotransferase (IU/L)	56.1 \pm 43.5	54.0 \pm 28.6	46.3 \pm 29.5
Prothrombin time (%)	91.5 \pm 14.8	73.4 \pm 9.7	77.7 \pm 15.4
Platelet ($\times 10^4$ /mm ³)	15.8 \pm 5.0	8.6 \pm 3.7	11.5 \pm 5.7
Albumin (g/dL)	4.0 \pm 0.3	3.5 \pm 0.4	3.5 \pm 0.5
Total bilirubin (mg/dL)	0.7 \pm 0.3	0.9 \pm 0.4	0.9 \pm 0.6
Child-Pugh grade: A/B	49/0	21/9	59/30
α -fetoprotein (ng/mL)	8.7 \pm 10.7	42.6 \pm 80.6	264.0 \pm 1281.7
TNM stage: I/II/III/IV			33/37/15/4
BCLC stage: A/B/C/D			44/13/26/6

BCLC, Barcelona-Clinic Liver Cancer; CH, chronic hepatitis; LC, liver cirrhosis; HCC, hepatocellular carcinoma.

were enrolled (Table 1). They were categorized into three groups according to the stage of the liver disease: chronic hepatitis (CH), liver cirrhosis (LC) and hepatocellular carcinoma (HCC). The clinical stage of HCC was determined according to the TNM classification system of the International Union against Cancer (7th edition) or the BCLC staging classification system. The protocol of this study was approved by the ethical committee of Osaka University Hospital and Osaka University Graduate School of Medicine. At enrollment, written informed consent was obtained from all patients and volunteers. Some of the HCC patients in this study received radiofrequency ablation (RFA) therapy based on the therapeutic guidelines for HCC promoted by the Japan Society of Hepatology.¹⁶ After the RFA sessions, the efficacy of tumor ablation or HCC recurrence was evaluated by computed tomography (CT) or magnetic resonance imaging (MRI) scanning. With some of the HCC patients who underwent surgical resection, cancerous and adjacent non-cancerous tissues were obtained at operation for further analyses of TEMs. As controls, we examined healthy subjects (HS) without history of liver disease, HCC patients with HBV infection (HBV-HCC group) and those without HBV or HCV (non-B, non-C [NBNC]-HCC group). The clinical backgrounds of the subjects are shown in Table 1.

Reagents

The fluorescence-labeled mouse or rat monoclonal antibodies against relevant molecules used in this study

Address reprint requests to: Tatsuya Kanto, M.D., Ph.D., Department of Gastroenterology and Hepatology, Osaka University Graduate School of Medicine, 2-2 Yamadaoka, Suita, 565-0871 Japan. E-mail: kantot@gb.med.osaka-u.ac.jp; fax: +81-6-6879-3629.

Copyright © 2013 by the American Association for the Study of Liver Diseases.

View this article online at wileyonlinelibrary.com.

DOI 10.1002/hep.25965

Potential conflict of interest: Nothing to report.

Additional Supporting Information may be found in the online version of this article.

were: CD14 (M5E2), CXCR4 (12G5), CD40 (5C3), CD16 (3G8), CD34 (5G3),

CD11b (ICRF44), CD49d (9F10), CD80 (L307.4), CD86 (2331), CD33 (WM53), CCR4 (1G1), HLA-DR (L243) and CCR5 (2D7/CCR5), which were purchased from Becton Dickinson (BD) Biosciences, San Jose, CA. Anti-human VEGFR2 (89106) or TIE2 (83715) Abs were purchased from R&D SYSTEMS, Minneapolis, MN; anti-human CD45 (HI30) from BioLegend, San Diego, CA; anti-human CX3CR1 (2A9-1) was from Medical & Biological Laboratories (MBL), Nagoya, Japan, and anti-AC133 (AC133) was from Miltenyi Biotec.

Phenotype and frequency analysis of peripheral and tumor-infiltrating TEMs

After peripheral blood mononuclear cells (PBMC) had been separated from heparinized venous blood by Ficoll-Hypaque (Nacalai tesque, Kyoto, Japan) density gradient centrifugation, they were stained with a combination of fluorescence-labeled anti-human mouse mAbs against CD14, CD16 and TIE2. For the analyses of liver-infiltrated cells, fresh liver specimens were washed twice with phosphate-buffered saline (PBS) and then diced into 5-mm pieces. After these pieces had been passed through a nylon mesh (BD Falcon, San Jose, CA), tumor-infiltrating and non-cancerous tissue-infiltrating leukocytes were isolated by density gradient centrifugation as described above. These cells were stained with fluorescence-labeled Abs (CD14, CD16 and TIE2) as done for PBMC. The stained cells were analyzed using FACS CantoII (BD) and FCS Express software (De Novo, Los Angeles, CA, USA).

Western-blot analysis

CD16+ and CD16- monocytes were sorted using a FACS sorter. The sorted cells (10^5 - 5×10^5) were subjected to Western blot analysis for TIE2 expression as described elsewhere.¹⁵

Immunofluorescence staining analysis

Tissue specimens were obtained from surgical resections of HCCs. Five-micrometer sections were fixed in 4% paraformaldehyde (PFA) for 15 minutes and immunostained. Briefly, the sections were incubated with the following antibodies by detection with a polymeric labeling 2-step method as described:¹⁵ rabbit anti-human CD14 antibody (clone, HPA001887; Sigma), mouse anti-human CD16 (2H7; MBL) and mouse anti-human TIE2 (AB33; Upstate Biotechnology) antibodies and subsequently with secondary goat anti-

rabbit Alexa Fluor[®]488 or goat anti-mouse Alexa Fluor[®]594 (Invitrogen, Molecular Probes) antibodies. Cell nuclei were counterstained with Dapi-Fluoromount-GTM (SouthernBiotech, Birmingham, AL). The stained tissues were analyzed by fluorescence microscopy (Model BZ-9000; Keyence, Osaka, Japan).

Immunohistochemical analysis and assessment of microvessel density

To evaluate microvessel density (MVD), immunohistochemical analyses were performed with anti-CD34 antibody (1/50 dilution; QB-END/10, Novo-castra, Newcastle, UK) using the avidin-biotin complex (ABC) method (Vectastain) as described.¹⁷

Single microvessels were detected as any brown CD34-immunostained endothelial cell structures. MVD was evaluated according to the method described by Poon et al.¹⁷ Sections were read by two double-blinded pathologists according to staining intensity.

Statistical analysis

Differences between two groups were assessed by the Mann-Whitney nonparametric U test, and multiple comparisons between more than two groups by the Kruskal-Wallis nonparametric test. Paired t tests were used to compare differences in paired samples using GraphPad Prism software (GraphPad Prism, San Diego, CA, USA). To differentiate HCC and LC, receiver operating characteristics (ROC) analyses were done using JMP software (SAS, Cary, NC, USA). The correlation between two groups was assessed by Pearson's analysis. The recurrence-free survival rate in patients with HCC who underwent the treatment was compared using the Kaplan-Meier method, with the log-rank test for comparison. Associations among the variables were determined by χ^2 test of Fisher exact test and Student t test. All tests were two-tailed, and a P value of less than 0.05 was considered statistically significant.

Results

TIE2 is selectively expressed on CD14+CD16+ monocytes

In order to examine which population of cells expresses TIE2, we stained PBMC obtained from HCC patients with relevant Abs. Among PBMC, CD14+HLA-DR+ monocytes we found to express TIE2 (Fig. 1A), whereas CD14-HLA-DR- cells did not (Fig. 1A). In particular, T-cells, B-cells, natural

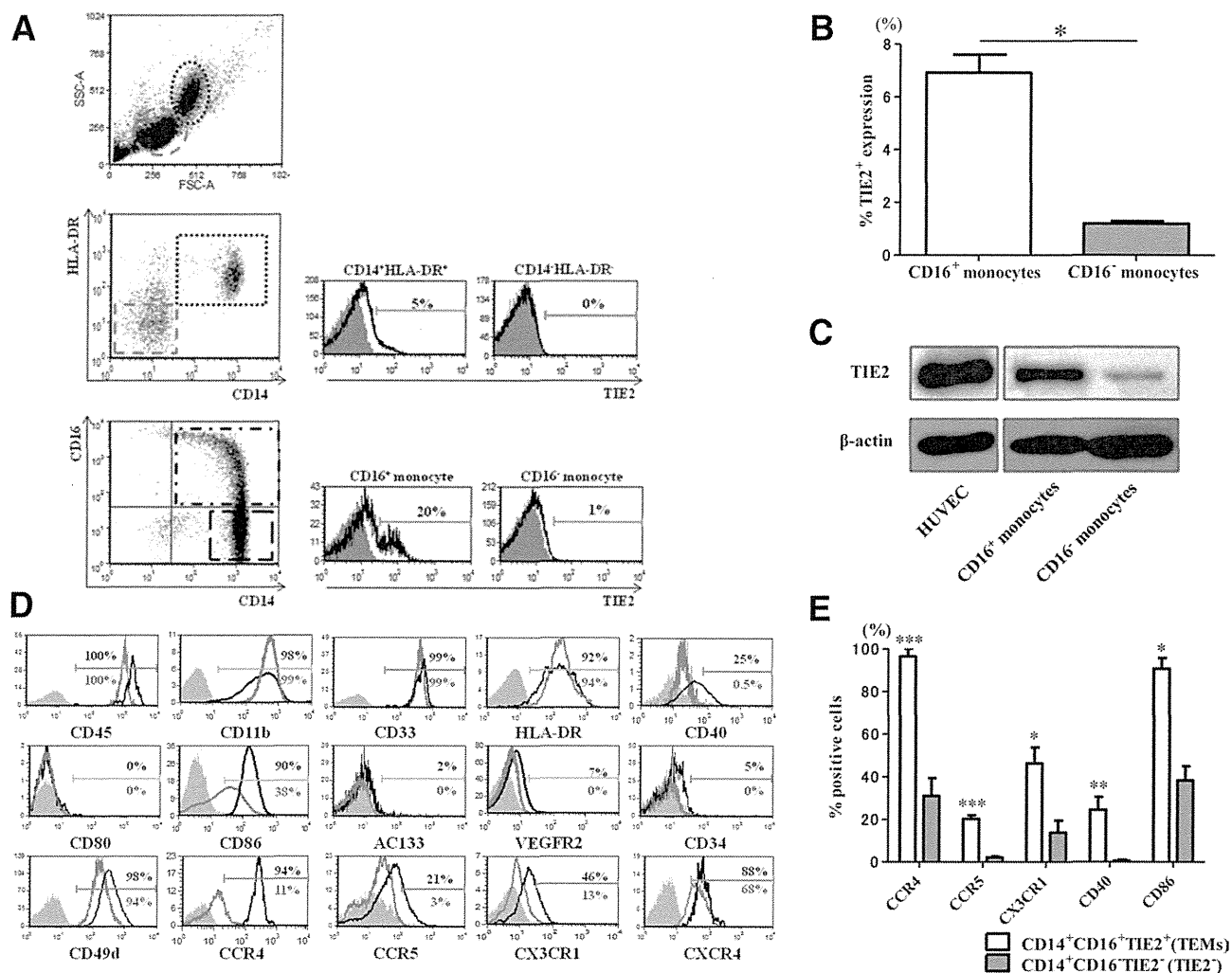


Fig. 1. Identification and phenotypic analyses of TEMs as CD14+CD16+TIE2+ cells in the peripheral blood. A. PBMC obtained from HCC patients were stained and analyzed by flow cytometry. CD14+ monocytes were divided into two distinct subsets, CD14++CD16- and CD14+CD16+ cells. These cells were examined for TIE2 expression. The numbers in the histograms depict the percentages of gated cells. Representative plots from three patients are shown. B. The frequency of TIE2+ cells in CD14+ monocytes was compared in the two monocyte subsets (CD16+ monocytes and CD16- monocytes; see Fig.1A). The bars indicate mean \pm SE in 89 patients. *: $p < 0.0001$ by Mann-Whitney nonparametric U test. C. Western-blot analysis of TIE2 expression in FACS-sorted CD14+CD16+ and CD14++CD16- cells from HCC patients. Bands correspond to TIE2 (140 kDa molecular weight; top panels) and P-actin (45 kDa molecular weight; bottom panels). The results are representative of three series of experiments from 7 HCC patients. D. TEMs and TIE2- monocytes in the peripheral blood were gated and analyzed for the expression of various cell surface markers, as indicated in the histogram plots. The filled light gray line, black line and gray line depict the negative control, the expression of relevant markers in TEMs and TIE2- monocytes, respectively. The percentage of the marker-positive cells is shown in the histograms. The upper numbers indicate TEMs; the lower numbers TIE2- monocytes. The plots are representative of six series of experiments. E. Comparative analysis of the expression of CCR4, CCR5, CX3CR1, CD40 and CD86 in TEMs and TIE2- monocytes, assessed by FACS as described above. The bars indicate mean \pm SE of six series of experiments. *: $p < 0.05$, **: $p < 0.005$, ***: $p < 0.001$ by Mann-Whitney non-parametric U test.

killer (NK) cells, NKT cells, and dendritic cells did not express detectable TIE2 (data not shown).

Monocytes can be divided into two distinct subsets according to the expression of CD14 and CD16: CD14++CD16- and CD14+CD16+ monocytes, respectively (Fig. 1A). CD14+CD16+ monocytes express TIE2 to a higher degree than CD14++CD16- monocytes (Fig. 1B). By Western blot analysis, TIE2 was expressed in CD14+CD16+ cells to a lesser extent than in HUVEC (used as a positive control);

however, TIE2 expression was higher in CD14+CD16+ than CD14++CD16- cells (Fig. 1C), in agreement with the flow cytometry data. From here on, we refer to CD14+CD16+TIE2+ cells as TIE2-expressing monocytes (TEMs).

TEMs are phenotypically and functionally distinct from TIE2- monocytes or endothelial progenitor cells in myeloid lineage

TEMs were found to express CD45, CD11b, CCR4, CCR5, CX3CR1, CD40 and CD86, the

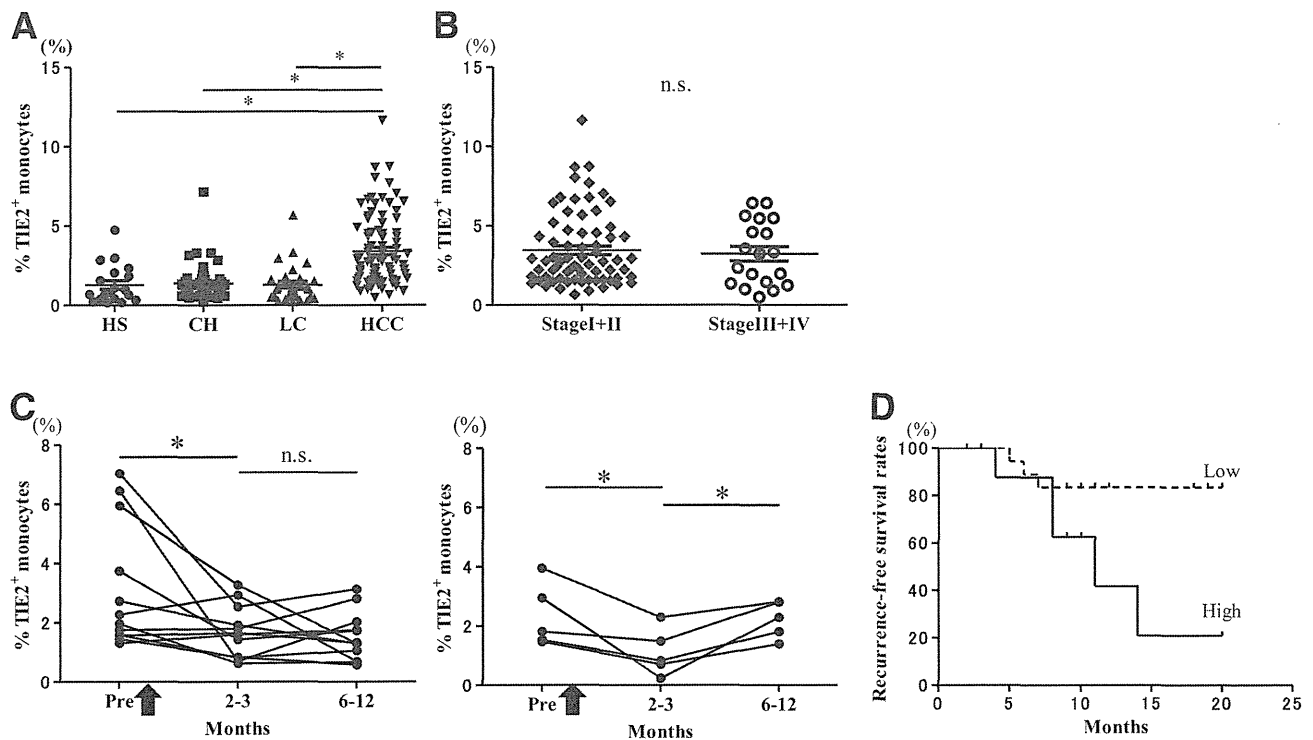


Fig. 2. Peripheral blood frequency of TEMs is increased in patients with HCC, with changes paralleling post-therapy HCC recurrence. A. The frequency of TEMs in CD14+ monocytes is shown in four groups of HCV-positive patients; HS, CH, LC and HCC, see Table 1. *: $p < 0.0001$ by Kruskal-Wallis test with Dunn's multiple comparison test. B. Frequency of TEMs in the blood of HCC patients at different clinical TNM stages (early stage; I+II; $n=70$, advanced stage; III+IV; $n=19$). n.s., not significant by Mann-Whitney nonparametric U test. C. In patients who underwent RFA therapy or resection of HCC, the frequency of TEMs among CD14+ monocytes was examined serially after confirmation of complete ablation or surgery to remove HCC lesions. The bold arrows depict the time point of RFA therapy or the operation. Both panels depict the frequency of TEMs in patients before and after treatment. The left panel shows TEM frequency in patients without HCC recurrence ($n=12$) as assessed by CT/MRI examinations, while the right panel shows TEM frequency in patients with HCC recurrence ($n=5$): *; $p < 0.05$ by Paired t-test. D. In HCC patients who underwent RFA or surgical resection, the recurrence-free survival rate after treatment was compared between patients with TEMhigh (frequency of TEMs $> 2.75\%$; $n=45$) and TEMlow (frequency of TEMs $< 2.75\%$; $n=44$) using the Kaplan-Meier method, with the log-rank test for comparison. TEMhigh and TEMlow, see Table 2. $p = 0.047$.

expression of which was generally higher than in TIE2- monocytes (Fig. 1D, 1E). The expression of CD33, HLA-DR, CD49d and CXCR4 was comparably high in monocytes regardless of CD16 or TIE2 expression. Since TEMs have been reported to be involved in the promotion of angiogenesis,^{4,13,18} we analyzed the expression of endothelial progenitor cell (EPC) markers.¹⁹ We found that TEMs do not express the EPC markers AC133, VEGFR2 or CD34 (Fig. 1D). Together, these results confirm that TEMs are phenotypically and functionally distinct from TIE2-monocytes or EPCs.

TEMs are significantly increased in the peripheral blood of HCC patients and their increase is associated with cancer occurrence and recurrence

We compared the frequency of TEMs in PBMC among healthy subjects and chronically HCV- infected patients with various stages of liver disease. With respect to the demographics of the subjects, no difference was found in the clinical and pathological characteristics among patient groups (Table 1). In HCC

patients, the frequency of TEMs in the blood was significantly higher than that in all other groups (Fig. 2A). However, the frequency of TEMs did not differ between patients at advanced HCC stages (TNM stages III and IV) and those at early HCC stages (stages I and II) (Fig. 2B). Similar results were obtained with the classification according to the BCLC staging system. Indeed, the frequency of TEMs did not differ between patients with advanced HCC stages (BCLC, C and D) and those with early stages (A and B) ($3.6 \pm 2.2\%$ vs. $3.3 \pm 2.3\%$). These results show that the increase of TEMs is closely related to the presence of HCC, irrespective of the stage of cancer. Furthermore, we observed higher TEM frequency in non- HCV-infected HCC patients (NBNC-, alcoholic- and HBV-HCC patients), than non-HCC subjects (Supplementary figure 1), suggesting that the increase of circulating TEMs is influenced by HCC, not by infection with hepatitis viruses.

We then serially examined the frequency of TEMs in HCC patients who underwent RFA therapy or

Table 2. Comparison of Clinical Parameters of HCC Patients Between Those with Higher Frequency of TEMs and Those with Lower Frequency

Clinicopathologic Characteristics	Peripheral TEMs		P
	High (n = 45)	Low (n = 44)	
Gender: male/female	32/13	31/13	1.000*
Age: mean \pm SD	71.4 \pm 6.6	68.7 \pm 7.3	0.065†
Child-Pugh grade: A/B	24/20	34/10	0.043*
MELD score	9.1 \pm 2.3	8.2 \pm 1.8	0.010‡
α -fetoprotein (ng/mL)	471.0 \pm 1785.2	52.3 \pm 101.4	0.101‡
TNM stage: I+II/III+IV	35/10	35/9	1.000*
BCLC stage: A+B/C+D	25/20	32/12	0.123*
Vascular invasion: present/absent	4/41	2/42	0.677*
Tumor size: <3/>3cm	36/9	34/10	0.800*
Tumor number: single/multiple	21/24	25/19	0.399*
Alanine aminotransferase (IU/L)	51.5 \pm 34.5	41.0 \pm 22.6	0.251‡
Prothrombin time (%)	73.3 \pm 14.5	82.6 \pm 15.0	0.004‡
Platelet ($\times 10^4$ /mm ³)	10.8 \pm 5.2	12.2 \pm 6.2	0.319‡
Albumin (g/dL)	3.4 \pm 0.4	3.6 \pm 0.6	0.045‡
Total bilirubin (mg/dL)	0.9 \pm 0.6	0.9 \pm 0.5	0.820‡

P < 0.05 in bold.

* χ^2 test or Fisher's exact test; †Student t test; ‡Mann-Whitney U test.
TEMs, TIE2-expressing monocytes; MELD, model for endstage liver disease.

tumor resection. We assessed the viability of HCC by CT or MRI scanning every 3 to 6 months after the treatment. In patients without HCC recurrence, the frequency of TEMs dramatically decreased after successful HCC ablation or resection (Fig. 2C). By contrast, in patients with subsequent HCC recurrence, TEMs increased before the apparent radiological identification of HCC (Fig. 2C). Therefore, TEM frequency dynamically changes in patients in correlation with the presence or recurrence of HCC.

In order to assess the clinical significance of TEMs as tumor biomarkers, we compared various clinical parameters in patients with either high or low TEM frequency. We fractionated HCC patients according to the frequency of circulating TEMs, defined as higher (TEM_{high}) or lower (TEM_{low}) than the median value (cut off value = 2.75%). We found that HCC patients in the TEM_{high} group displayed (i) a more advanced Child-Pugh grade (B); (ii) a higher model for endstage liver disease (MELD) score; (iii) a lower prothrombin time; (iv) a lower serum albumin level (Table 2). These results suggest that elevated TEM frequency in the peripheral blood is associated with a deterioration of liver function in HCC patients. Furthermore, patients in the TEM_{high} group showed significantly shorter recurrence-free survival rates than those in the TEM_{low} group (assessed before RFA treatment or resection of HCC), suggesting that the assessment of TEM frequency in the blood holds prognostic value (Fig. 2D)

TEMs are located in the perivascular areas of HCC

We found that most TEMs, identified as CD14+TIE2+ cells by immunofluorescence staining, were located in the perivascular areas of HCC (Fig. 3A-[A], [B], [D]). Most of the CD16+ cells co-stained with CD14+TIE2+ cells (Fig. 3A-[C]). Some of the TEMs were observed in the lumen of intra-tumoral blood vessels, identified as CD14-TIE2+ vascular structures (Fig. 3A-[D]). However, TEMs were scarce in the adjacent non-cancerous liver tissue (not shown).

TEMs accumulate in HCC tissue

The frequency of TEMs among tumor-infiltrating leukocytes (TIL) was higher than nontumor-infiltrating leukocytes (NIL) and PBMC (Fig. 3B), suggesting that TEMs preferentially accumulate in the HCC tissue as compared with normal liver tissue. Moreover, in patients with HCC, the frequency of TEMs in PBMCs correlated with that in TIL (Fig. 3C), suggesting that TEM frequency in the blood may represent a surrogate biomarker of TEM infiltration in the tumors.

TEM frequency correlates with microvessel density (MVD) in HCC

To study whether the frequency of circulating and intra-hepatic TEMs correlate with tumor angiogenesis, we measured microvascular density by anti-CD34 staining in liver tissue obtained from 12 HCC patients. The expression of CD34 was predominantly confined to the cytoplasm of vascular endothelial cells. Microvessels were identified as brown/yellow capillaries or small cell clusters. The CD34+ microvessels were located mainly in tumor cell areas (Fig. 4A). MVD tended to be higher in HCC (67.0 \pm 57.8) than in non-cirrhotic (26.7 \pm 7.5) or cirrhotic non-cancerous tissues (32.1 \pm 11.6). Furthermore, MVD in HCC correlated with both circulating and

intra-hepatic TEM frequency (Fig. 4B). These results might suggest that TEMs are involved in the promotion of neo-vascularization in HCC.

Blood TEM frequency is superior to AFP and PIVKA-II serum levels as diagnostic marker in HCC

In order to evaluate the significance of TEM frequency as a diagnostic marker of HCC, we examined whether TEM frequency correlates with various clinical parameters in HCC patients. No correlation was found between TEM frequency and other HCC-specific markers such as α -fetoprotein (AFP) or protein induced by the absence of vitamin K or antagonist II (PIVKA-II)

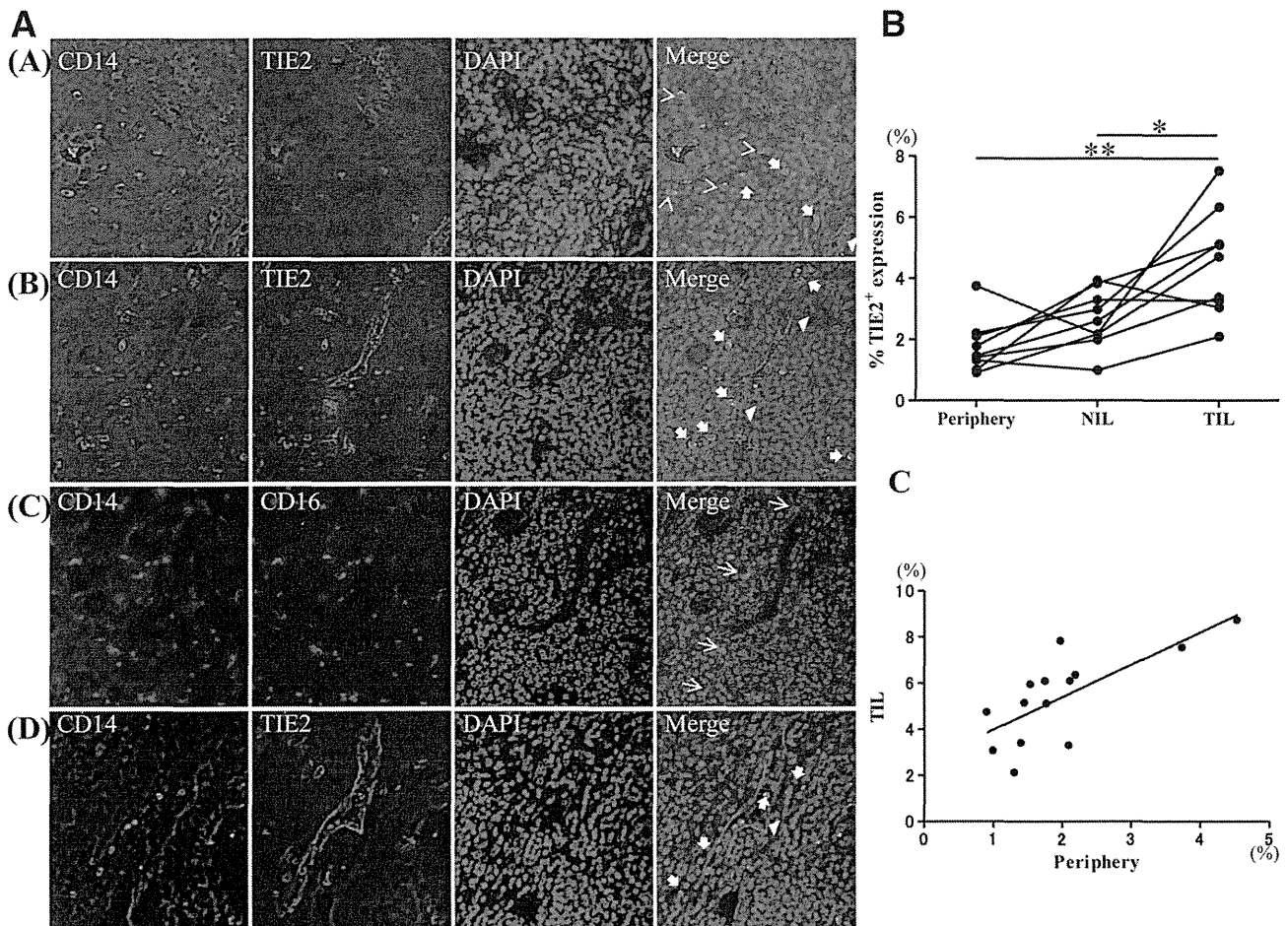


Fig. 3. TEMs are observed in perivascular areas of HCC tissue, and their frequency is higher in HCC tissue than in the peripheral blood. A. Immunofluorescence staining of CD14 (green), CD16 (red) and TIE2 (red) identifies CD14+TIE2-, CD14+TIE2+, CD14+CD16- and CD14+CD16+ monocytes in human liver tissue (blue: nuclei counterstained with Dapi). Representative results of the resected samples obtained from 12 HCC patients are shown. The panels show CD14+TIE2+ TEMs (A, B, D) and CD14+CD16+ cells (C) in the perivascular areas of HCC (magnification, 400x). Bold arrows depict CD14+TIE2+ TEMs; thin arrows depict CD14+CD16+ cells; bold arrowheads depict TIE2+CD14- blood vessels; and thin arrowheads depict CD14+TIE2- cells. B. The frequency of TEMs in 9 patients with HCC was assessed in the peripheral blood and in liver tissue. Liver-infiltrating leukocytes are divided into two distinct groups: leukocytes infiltrating non-tumor tissue (NIL) and tumor-infiltrating leukocytes (TIL). Cells were stained using anti-human CD14, CD16 and TIE2 mAbs. The samples were obtained from 9 patients who underwent tumor resection. *: p<0.05, **: p<0.0005, by Paired t-test. C. Correlation between the frequency of TEMs in PBMC and tumor-infiltrated lymphocytes. The analysis (n=14) was based on Pearson's correlation coefficient. P = 0.003, R2 = 0.53.

(Fig. 5A). In addition, circulating TEM frequency did not correlate with the levels of examined angiogenic factors, such as VEGF, ANG-2, sVEGFR-1 and MIF (Supplementary figure 2). As for the diagnostic value of TEM frequency for differentiating HCC from chronic liver disease (CLD; chronic hepatitis and liver cirrhosis patients) or liver cirrhosis, its sensitivity and specificity were 86.1 and 71% and 81.3 and 90%, respectively (Table 3). ROC analyses revealed that TEM frequency was superior to AFP, PIVKA-II and ANG-2 levels as a diagnostic marker for HCC (Fig. 5B and Table 3).

Discussion

In this study, we defined TEMs as CD14+CD16+TIE2+ cells and examined their frequency, localization

and correlation with micro-vessel density in HCC. We show that: (i) TEM frequency is significantly increased both in PBMC and tumors of HCC patients, and positively correlates with MVD in the HCC tissue; (ii) TEM frequency dynamically changes in relation to tumor ablation or recurrence; (iii) The frequency of TEMs in the peripheral blood may serve as a better diagnostic marker of HCC than AFP, PIVKA-II and ANG-2 serum levels. These results may suggest that certain HCC-derived factors stimulate the differentiation of TEMs, whose abundance in HCC correlates with the degree of vascular density.

According to the pattern of CD16 and CD14 expression, it has been reported that monocytes can be categorized into distinct subsets, such as classical (CD14+CD16-) and non-classical monocytes

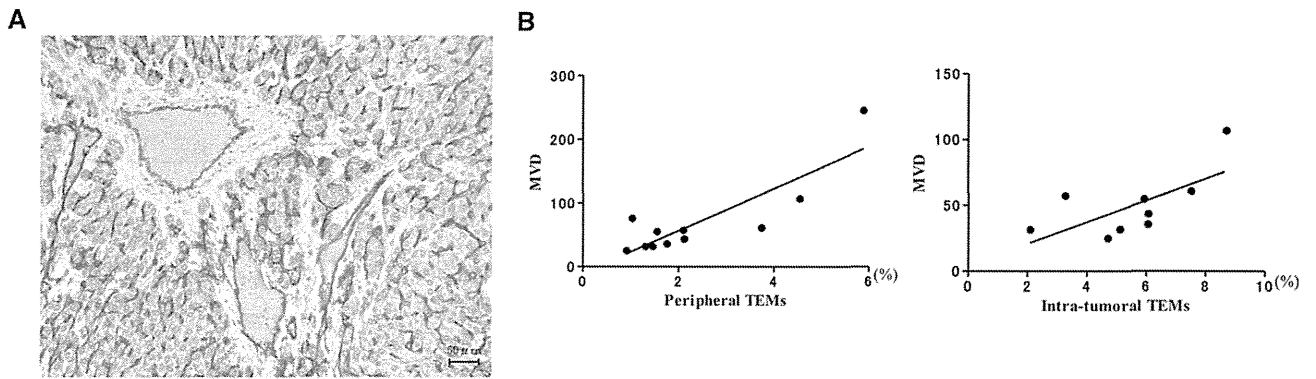


Fig. 4. The degree of MVD in HCC correlates with the frequency of TEMs A. Assessment of angiogenesis in HCC was performed by immunostaining of CD34 in resected samples obtained from patients with HCC. Microvessels are shown by the brown/yellow staining of capillaries or small cell clusters. Representative results are shown. The panel shows a tumor cell area of a high grade tumor. B. Correlation between TEM frequency and MVD in HCC patients. The panels show the correlation of peripheral blood (left: n=11) or intra-tumoral (right: n=9) TEM frequency and MVD (p = 0.0009, R2 = 0.72 and p = 0.04, R2 = 0.44, respectively). Analysis was based on Pearson's correlation coefficient.

(CD14+CD16+).²⁰ Such populations are regarded as functionally distinct, since the frequency of CD14+CD16+ cells predominantly increases under inflammatory conditions such as chronic hepatitis and inflammatory bowel disease.^{21,22} We identified TEMs within the CD14+CD16+ monocyte subset, suggesting that TIE2 is predominantly expressed/induced in the CD16+ monocytes. However, the precise mechanisms regulating TIE2 induction in monocytes remain largely unknown. Furthermore, it is yet to be clarified whether CD16+ monocytes derive from CD16-

monocytes. Multiple factors are reported to enhance CD16 expression on monocytes, such as macrophage-colony-stimulating factor (M-CSF), IL-10 and transforming growth factor (TGF)-B1.²³ Recent studies have suggested that hypoxia and MIF increase TIE2 expression on monocytes in vitro.^{14,24} Cumulative data have been published showing that cancer cells, including HCC, are dichotomously capable of releasing various inflammatory (TNF- α , IL-1P) and anti-inflammatory (TGF-P and IL-10) cytokines, as well as hematopoietic factors (M-CSF and MIF).^{7,25-29}

Fig. 5. TEM frequency is superior, as a diagnostic marker for HCC relative to other tumor/angiogenesis parameters. A. Correlation between TEM frequency and AFP (n=87) or PIVKA-II (n=81) analyzed by Pearson's correlation coefficient. P = 0.45, R2 = 0.007 or P = 0.27, R2 = 0.02, respectively. B. ROC analyses were performed in order to assess the diagnostic value of TEM frequency for differentiating HCC (n=89) from chronic liver disease (CLD, n=79) or liver cirrhosis (LC, n=30). The left panel shows the diagnostic value of TEMs, PIVKA-II, AFP and ANG-2 for HCC (compared with CLD); the right panel shows the diagnostic value of TEMs, PIVKA-II, AFP and ANG-2 for HCC (compared with LC).

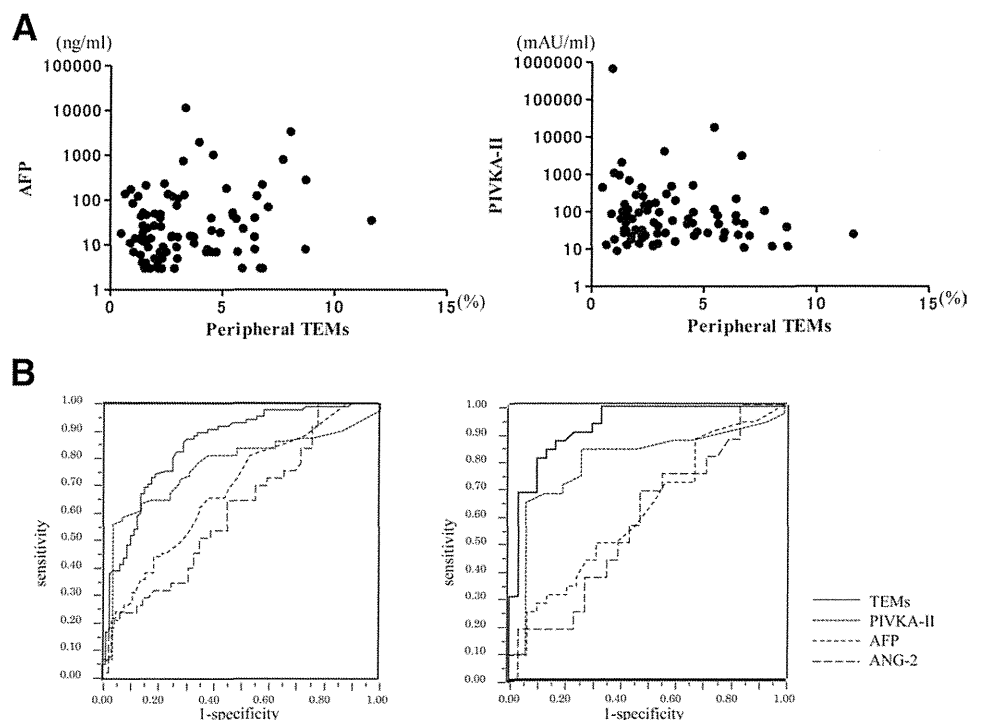


Table 3. Assessment of Diagnostic Value of TEMs, AFP, and PIVKA-II by ROC Analyses

Discrimination Between	Parameter	AUC	Cutoff Value	Sensitivity (%)	Specificity (%)	Positive Predictive Values (%)	Negative Predictive Values (%)
HCC and CLD	TEMs	0.85	1.46	86.1	71	76.3	82.4
	AFP	0.69	10	65.9	43.9	65.9	56.1
	PIVKA-II	0.77	47	56.3	96.5	97.8	44.5
	ANG-2	0.62	2681	51.4	67.3	52.8	64
HCC and LC	TEMs	0.93	2.75	81.3	90	89.7	81.8
	AFP	0.61	10	71.9	32.1	54.8	50
	PIVKA-II	0.79	39	64.5	93.3	95.2	56
	ANG-2	0.57	2440	68.8	52	47.8	72.2

The optimal cutoff point was determined as those yielding the minimal value for $(1 - \text{sensitivity})^2 + (1 - \text{specificity})^2$. Such points with those sensitivity and specificity values are the closest to the (0, 1) point on the ROC curve.

AUC, area under the curve; TEMs, TIE2-expressing monocytes; CLD, chronic liver disease; LC, liver cirrhosis; ANG-2, angiopoietin-2.

However, no correlation was found between the frequency of TEMs and that of angiogenesis factors in the serum of HCC patients (Supplementary figure 2). It is thus plausible that a combination of HCC-derived factors contributes to the induction/expansion of TEMs, as suggested by preliminary studies (manuscript in preparation).

Although the presence of TEMs has been reported in cancer tissues from patients with colorectal, pancreatic or renal cancer,¹⁵ the actual role of TEMs in the angiogenic process of HCC remains to be elucidated. In this study, we showed that blood and intra-hepatic frequency of TEMs positively correlate with the density of microvascular structures in the liver. Additionally, we found that TEMs accumulate in the liver and are mostly located in the perivascular HCC areas. In support to our observations, Venneri et al. reported that TEMs preferentially localize in the vicinity of tumor blood vessels in human cancer specimens, but are not found in non-neoplastic tissues adjacent to tumors.¹⁵ These results suggest that TEMs may have a role in HCC-induced angiogenesis. Further studies are now needed to identify the molecular mechanisms that regulate TEM accumulation in the liver. Interactions between chemokine and their receptors, such as CCR5 or CX3CR1 (which are expressed in TEMs), may be involved in such process.²²

Thus far, many studies have reported that the histological degree of angiogenesis in the liver closely correlates with prognosis or survival of HCC patients. Accordingly, several serum angiogenesis factors, such as VEGF, ANG-2, sVEGFR-1 and MIF, were reported as markers of prognosis, invasiveness and/or post-therapeutic recurrence in HCC patients.⁷⁻¹¹ Multivariate analysis showed that the degree of angiogenesis in the liver, as assessed by MVD, is an independent predictive factor for disease-free survival in patients with resectable HCC.¹⁷ Therefore, the positive correlation

between circulating/intra-hepatic TEM frequency and MVD in the liver observed in our supports the notion that TEMs could represent a prognostic marker in HCC patients. In support of this, we found that patients with higher TEM frequency were at a more advanced Child-Pugh stage, had poorer liver function and showed higher rate of post-therapy recurrence.

In order to diagnose HCC, serum AFP and PIVKA-II levels have been commonly used in the clinical practice. However, the sensitivity and specificity of both markers are unsatisfactory for the detection of HCC.¹² In the present study, ROC analysis revealed that the frequency of TEMs in the peripheral blood has higher sensitivity and specificity than serum AFP, PIVKA-II, ANG-2 levels in differentiating HCC from CLD or LC. However, evaluation of the clinical value of TEMs in the long-term prognosis of HCC patients is needed as the observation periods in the current study were limited to a maximum of 2 years.

In summary, we found that TEMs are significantly increased both in the peripheral blood and liver of HCC patients, thus holding diagnostic value for HCC. Furthermore, the frequency of TEMs correlated with the degree of angiogenesis in HCC tissue. Thus, TEMs might represent a novel diagnostic cellular marker for HCC, potentially reflecting angiogenesis in the liver.

References

1. Parkin DM, Bray F, Ferlay J, Pisani P. Estimating the world cancer burden: Globocan 2000. *Int J Cancer* 2001;94:153-156.
2. El-Serag HB. Hepatocellular carcinoma: recent trends in the United States. *Gastroenterology* 2004;127:S27-S34.
3. Llovet JM, Burroughs A, Bruix J. Hepatocellular carcinoma. *Lancet* 2003;362:1907-1917.
4. Murdoch C, Muthana M, Coffelt SB, Lewis CE. The role of myeloid cells in the promotion of tumour angiogenesis. *Nat Rev Cancer* 2008; 8:618-631.
5. El-Assal ON, Yamanoi A, Soda Y, Yamaguchi M, Igarashi M, Yamamoto A, et al. Clinical significance of microvessel density and vascular

- endothelial growth factor expression in hepatocellular carcinoma and surrounding liver: possible involvement of vascular endothelial growth factor in the angiogenesis of cirrhotic liver. *HEPATOLOGY* 1998;27:1554-1562.
6. Coulon S, Heindryckx F, Geerts A, Van Steenkiste C, Colle I, Van Vlierberghe H. Angiogenesis in chronic liver disease and its complications. *Liver Int* 2011;31:146-162.
 7. Hira E, Ono T, Dhar DK, El-Assal ON, Hishikawa Y, Yamanoi A, et al. Overexpression of macrophage migration inhibitory factor induces angiogenesis and deteriorates prognosis after radical resection for hepatocellular carcinoma. *Cancer* 2005;103:588-598.
 8. Kuboki S, Shimizu H, Mitsuhashi N, Kusashio K, Kimura F, Yoshidome H, et al. Angiopoietin-2 levels in the hepatic vein as a useful predictor of tumor invasiveness and prognosis in human hepatocellular carcinoma. *J Gastroenterol Hepatol* 2008;23:e157-164.
 9. Nagaoka S, Yoshida T, Akiyoshi J, Akiba J, Hisamoto T, Yoshida Y, et al. The ratio of serum placenta growth factor to soluble vascular endothelial growth factor receptor-1 predicts the prognosis of hepatocellular carcinoma. *Oncol Rep* 2010;23:1647-1654.
 10. Schoenleber SJ, Kurtz DM, Talwalkar JA, Roberts LR, Gores GJ. Prognostic role of vascular endothelial growth factor in hepatocellular carcinoma: systematic review and meta-analysis. *Br J Cancer* 2009;100:1385-1392.
 11. Tamesa T, Iizuka N, Mori N, Okada T, Takemoto N, Tangoku A, et al. High serum levels of vascular endothelial growth factor after hepatectomy are associated with poor prognosis in hepatocellular carcinoma. *Hepatogastroenterology* 2009;56:1122-1126.
 12. Yuen MF, Lai CL. Serological markers of liver cancer. *Best Pract Res Clin Gastroenterol* 2005;19:91-99.
 13. De Palma M, Venneri MA, Galli R, Sergi L, Politi LS, Sampaolesi M, et al. Tie2 identifies a hematopoietic lineage of proangiogenic monocytes required for tumor vessel formation and a mesenchymal population of pericyte progenitors. *Cancer Cell* 2005;8:211-226.
 14. Murdoch C, Tazzyman S, Webster S, Lewis CE. Expression of Tie-2 by human monocytes and their responses to angiopoietin-2. *J Immunol* 2007;178:7405-7411.
 15. Venneri MA, De Palma M, Ponzoni M, Pucci F, Scielzo C, Zonari E, et al. Identification of proangiogenic TIE2-expressing monocytes (TEMs) in human peripheral blood and cancer. *Blood* 2007;109:5276-5285.
 16. Clinical Practice Guidelines for Hepatocellular Carcinoma — The Japan Society of Hepatology 2009 update. *Hepatol Res* 2010;40(Suppl 1):2-144.
 17. Poon RT, Ng IO, Lau C, Yu WC, Yang ZF, Fan ST, et al. Tumor microvessel density as a predictor of recurrence after resection of hepatocellular carcinoma: a prospective study. *J Clin Oncol* 2002;20:1775-1785.
 18. Coffelt SB, Tal AO, Scholz A, De Palma M, Patel S, Urbich C, et al. Angiopoietin-2 regulates gene expression in TIE2-expressing monocytes and augments their inherent proangiogenic functions. *Cancer Res* 2010;70:5270-5280.
 19. Mund JA, Case J. The ontogeny of endothelial progenitor cells through flow cytometry. *Curr Opin Hematol* 2011;18:166-170.
 20. Ancuta P, Liu KY, Misra V, Wacleche VS, Gosselin A, Zhou X, et al. Transcriptional profiling reveals developmental relationship and distinct biological functions of CD16+ and CD16- monocyte subsets. *BMC Genomics* 2009;10:403.
 21. Koch S, Kucharzik T, Heidemann J, Nusrat A, Luegering A. Investigating the role of proinflammatory CD16+ monocytes in the pathogenesis of inflammatory bowel disease. *Clin Exp Immunol* 2010;161:332-341.
 22. Zimmermann HW, Seidler S, Nattermann J, Gassler N, Hellerbrand C, Zerneck A, et al. Functional contribution of elevated circulating and hepatic non-classical CD14CD16 monocytes to inflammation and human liver fibrosis. *PLoS One* 2010;5:e11049.
 23. Iwahashi M, Yamamura M, Aita T, Okamoto A, Ueno A, Ogawa N, et al. Expression of Toll-like receptor 2 on CD16+ blood monocytes and synovial tissue macrophages in rheumatoid arthritis. *Arthritis Rheum* 2004;50:1457-1467.
 24. Schoenfeld J, Jinushi M, Nakazaki Y, Wiener D, Park J, Soiffer R, et al. Active immunotherapy induces antibody responses that target tumor angiogenesis. *Cancer Res* 2010;70:10150-10160.
 25. Hsia CY, Huo TI, Chiang SY, Lu MF, Sun CL, Wu JC, et al. Evaluation of interleukin-6, interleukin-10 and human hepatocyte growth factor as tumor markers for hepatocellular carcinoma. *Eur J Surg Oncol* 2007;33:208-212.
 26. Laurent J, Touvrey C, Botta F, Kuonen F, Ruegg C. Emerging paradigms and questions on pro-angiogenic bone marrow-derived myelomonocytic cells. *Int J Dev Biol* 2011;55:527-534.
 27. Song BC, Chung YH, Kim JA, Choi WB, Suh DD, Pyo SI, et al. Transforming growth factor-beta1 as a useful serologic marker of small hepatocellular carcinoma. *Cancer* 2002;94:175-180.
 28. Talaat RM. Soluble angiogenesis factors in sera of Egyptian patients with hepatitis C virus infection: correlation with disease severity. *Viral Immunol* 2010;23:151-157.
 29. Zhu XD, Zhang JB, Zhuang PY, Zhu HG, Zhang W, Xiong YQ, et al. High expression of macrophage colony-stimulating factor in peritumoral liver tissue is associated with poor survival after curative resection of hepatocellular carcinoma. *J Clin Oncol* 2008;26:2707-2716.

The Bcl-2 Homology Domain 3 (BH3)-only Proteins Bim and Bid Are Functionally Active and Restrained by Anti-apoptotic Bcl-2 Family Proteins in Healthy Liver^{*[S]}

Received for publication, December 7, 2012, and in revised form, August 21, 2013. Published, JBC Papers in Press, August 28, 2013, DOI 10.1074/jbc.M112.443093

Takahiro Kodama, Hayato Hikita, Tsukasa Kawaguchi, Yoshinobu Saito, Satoshi Tanaka, Minoru Shigekawa, Satoshi Shimizu, Wei Li, Takuya Miyagi, Tatsuya Kanto, Naoki Hiramatsu, Tomohide Tatsumi, and Tetsuo Takehara¹

From the Department of Gastroenterology and Hepatology, Osaka University Graduate School of Medicine, 2-2 Yamada-oka, Suita, Osaka 565-0871, Japan

Background: A fine balance between the anti- and pro-apoptotic multidomain Bcl-2 family proteins controls hepatocyte apoptosis in the healthy liver.

Results: Disruption of the BH3-only proteins Bim and Bid prevents spontaneous hepatocyte apoptosis in the absence of anti-apoptotic Bcl-2 family proteins.

Conclusion: Hepatocyte integrity is maintained by the well orchestrated Bcl-2 network.

Significance: We demonstrated the novel involvement of BH3-only proteins in the healthy Bcl-2 network of the liver.

An intrinsic pathway of apoptosis is regulated by the B-cell lymphoma-2 (Bcl-2) family proteins. We previously reported that a fine rheostatic balance between the anti- and pro-apoptotic multidomain Bcl-2 family proteins controls hepatocyte apoptosis in the healthy liver. The Bcl-2 homology domain 3 (BH3)-only proteins set this rheostatic balance toward apoptosis upon activation in the diseased liver. However, their involvement in healthy Bcl-2 rheostasis remains unknown. In the present study, we focused on two BH3-only proteins, Bim and Bid, and we clarified the Bcl-2 network that governs hepatocyte life and death in the healthy liver. We generated hepatocyte-specific Bcl-xL- or Mcl-1-knock-out mice, with or without disrupting Bim and/or Bid, and we examined hepatocyte apoptosis under physiological conditions. We also examined the effect of both Bid and Bim disruption on the hepatocyte apoptosis caused by the inhibition of Bcl-xL and Mcl-1. Spontaneous hepatocyte apoptosis in Bcl-xL- or Mcl-1-knock-out mice was significantly ameliorated by Bim deletion. The disruption of both Bim and Bid completely prevented hepatocyte apoptosis in Bcl-xL-knock-out mice and weakened massive hepatocyte apoptosis via the additional *in vivo* knockdown of *mcl-1* in these mice. Finally, the hepatocyte apoptosis caused by ABT-737, which is a Bcl-xL/Bcl-2/Bcl-w inhibitor, was completely prevented in Bim/Bid double knock-out mice. The BH3-only proteins Bim and Bid are functionally active but are restrained by the anti-apoptotic Bcl-2 family proteins under physiological conditions. Hepatocyte integrity is maintained by the dynamic and well orchestrated Bcl-2 network in the healthy liver.

These members are divided into two groups as follows: core Bcl-2 family proteins, which possess three or four Bcl-2 homology domains (BH1–BH4)² and the Bcl-2 homology domain 3 (BH3)-only proteins (1). The former, which are multidomain proteins, are subdivided into pro- and anti-apoptotic proteins. Pro-apoptotic core Bcl-2 family members, such as Bax and Bak, serve as effector molecules of this apoptotic machinery. Upon activation, these members can form pores to permeabilize the mitochondrial outer membrane. Apoptogenic factors, such as cytochrome *c*, can then be released through this membrane into the cytosol, leading to the activation of the caspase cascade and to cellular demise (2). Anti-apoptotic core Bcl-2 family members, including Bcl-2, Bcl-xL, Mcl-1, Bcl-w, and Bfl-1/A1, inhibit the intrinsic pathway of apoptosis by either directly or indirectly antagonizing Bak/Bax activity (3–5). In the original rheostasis model, cellular life and death are regulated by a balance between these anti- and pro-apoptotic core Bcl-2 family proteins (6). We previously reported that the hepatocyte-specific deletion of the *bcl-x* gene resulted in spontaneous hepatocyte apoptosis, and this effect could be completely prevented by the additional deletion of the *bak* and *bax* genes (7). These findings elucidated the importance of the rheostatic balance of the core Bcl-2 family proteins in controlling hepatocyte apoptosis in the healthy liver.

The BH3-only proteins, which include at least eight members, are considered to function as pro-apoptotic sensors, and these proteins set this rheostatic balance toward apoptosis upon activation by a variety of apoptotic stimuli (8, 9). It has been reported that hepatocyte apoptosis through the activation of these BH3-only proteins is involved in the pathophysiology of various liver diseases (10–12). Alternatively, we previously reported that the slight activation of Bid, which can trigger hepatocyte apoptosis, occurs even in the healthy liver and that the inactivation of Bid partially ameliorated spontaneous hepato-

Apoptosis via the intrinsic pathway, which is known as the mitochondrial pathway, is regulated by Bcl-2 family members.

* This work was supported in part by a grant-in-aid for scientific research from the Ministry of Education, Culture, Sports, Science, and Technology of Japan (to T. Takehara).

[S] This article contains supplemental Figs. 1–4.

¹ To whom correspondence should be addressed. Tel.: 81-6-6879-3621; Fax: 81-6-6879-3629; E-mail: takehara@gh.med.osaka-u.ac.jp.

² The abbreviations used are: BH1–BH4, Bcl-2 homology domains 1–4; SCID, severe combined immune deficiency; ALT, alanine aminotransferase.

The Novel Bcl-2 Network in Healthy Liver

cyte apoptosis in Bcl-xL- or Mcl-1-knock-out mice (7, 13). In the present study, we focused on another BH3-only protein, Bim, which promotes hepatocyte apoptosis upon activation by free fatty acids or by reactive oxygen species in pathological settings, and we further clarified the orchestration of the Bcl-2 network, which governs hepatocyte life and death in the physiological state (10, 11, 14, 15). We found that the disruption of Bim ameliorated hepatocyte apoptosis in Bcl-xL- or Mcl-1-knock-out mice, indicating the involvement of Bim in this hepatocyte apoptosis machinery in the healthy liver as well as that of Bid. Additionally, the deletion of both Bim and Bid prevented the massive hepatocyte apoptosis caused by the inhibition of both Bcl-xL and Mcl-1, suggesting that Bim and Bid are functionally active in the healthy liver and are essential regulators for promoting the intrinsic pathway of apoptosis in hepatocytes in the absence of anti-apoptotic Bcl-2 family proteins. Our present study unveiled the fine and dynamic Bcl-2 networks, the orchestration of which determines hepatocyte life and death in the healthy liver.

EXPERIMENTAL PROCEDURES

Mice—Mice carrying a *bcl-x* gene with two *loxP* sequences at the promoter region and a second intron (*bcl-x^{lox/lox}*), mice carrying an *mcl-1* gene encoding amino acids 1–179 flanked by two *loxP* sequences, and heterozygous *alb-cre* transgenic mice expressing the Cre recombinase gene under regulation of the *albumin* gene promoter have been described previously (16–18). Hepatocyte-specific Bcl-xL-knock-out mice (*bcl-x^{lox/lox}alb-cre*) (17), hepatocyte-specific Mcl-1-knock-out mice (*bcl-x^{lox/lox}alb-cre*) (13), systemic Bid-knock-out mice (*bid^{-/-}*) (12), and Bcl-xL/Bid double knock-out mice (*bid^{-/-}bcl-x^{lox/lox}alb-cre*) (7) have also been described previously. We purchased C57BL/6J mice from Charles River (Osaka, Japan), systemic Bim-knock-out mice (*bim^{-/-}*) from the Jackson Laboratory (Bar Harbor, ME), and NOD/ShiJic-*scid* Jcl mice from Clea Japan Inc. (Osaka, Japan). We generated Bcl-xL/Bim double knock-out mice (*bim^{-/-}bcl-x^{lox/lox}alb-cre*), Mcl-1/Bim double knock-out mice (*bim^{-/-}mcl-1^{lox/lox}alb-cre*), Bcl-xL/Bim/Bid triple knock-out mice (*bim^{-/-}bid^{-/-}bcl-x^{lox/lox}alb-cre*), and Bim/Bid double knock-out mice (*bim^{-/-}bid^{-/-}*) by mating the strains. We generated mice with a hepatocyte-specific deletion of Mcl-1 and homozygote severe combined immune deficiency (SCID) mutations (*mcl-1^{lox/lox}prkdc^{scid/scid}alb-cre*) by mating hepatocyte-specific Mcl-1-knock-out mice (*bcl-x^{lox/lox}alb-cre*) and NOD/ShiJic-*scid* Jcl mice. Genotyping of *prkdc^{scid}* gene mutation was performed by the PCR-confronting two-pair primer (PCR-CTPP) method reported previously (19). The mice were maintained in a specific pathogen-free facility and were afforded humane care under approval from the Animal Care and Use Committee of Osaka University Medical School.

Histological Analyses—Liver sections were stained with hematoxylin and eosin (H&E). To detect apoptotic cells, the liver sections were also subjected to staining by terminal deoxynucleotidyltransferase-mediated deoxyuridine triphosphate nick-end labeling (TUNEL) according to a procedure reported previously (20). For immunohistochemical detection of cleaved caspase-3, the liver sections were incubated with the

polyclonal rabbit anti-cleaved caspase-3 antibody (Cell Signaling Technology, Beverly, MA) according to a procedure reported previously (20).

Caspase-3/7 Activity—Serum caspase-3/7 activity was measured by a luminescent substrate assay for caspase-3 and caspase-7 (Caspase-Glo assay, Promega) according to the manufacturer's protocol.

Western Blot Analysis—Liver tissue was lysed in lysis buffer (1% Nonidet P-40, 0.5% sodium deoxycholate, 0.1% SDS, 1× protein inhibitor mixture (Nacalai tesque, Kyoto, Japan), 1× phosphatase inhibitor mixture (Nacalai tesque), and phosphate-buffered saline, pH 7.4). The liver lysates were cleared by centrifugation at $10,000 \times g$ for 15 min at 4 °C. The protein concentrations were determined using a bicinchoninic acid protein assay kit (Pierce). The protein lysates were electrophoretically separated with SDS-polyacrylamide gels and were transferred onto a polyvinylidene fluoride membrane. For immunodetection, the following antibodies were used: a rabbit polyclonal antibody to Bcl-xL (Santa Cruz Biotechnology, Inc.), a rabbit polyclonal antibody to Bid, a rabbit polyclonal antibody to Bax, a rabbit polyclonal antibody to cleaved caspase-3, a rabbit polyclonal antibody to cleaved caspase-7, a rabbit polyclonal antibody to Puma (Cell Signaling Technology, Beverly, MA), a rabbit monoclonal antibody to Bad, a rabbit polyclonal antibody to Noxa (Abcam, Cambridge, MA), a rabbit polyclonal antibody to Bak (Millipore, Billerica, MA), a rabbit polyclonal antibody to Bim (Enzo Life Sciences Inc., Farmingdale, NY), a rabbit polyclonal antibody to Mcl-1 (Rockland, Gilbertsville, PA), and a mouse monoclonal antibody to β -actin (Sigma-Aldrich).

Real-time Reverse Transcription Polymerase Chain Reaction (Real-time RT-PCR) for mRNA—Total RNA was extracted from liver tissues using an RNeasy minikit (Qiagen, Valencia, CA), was reverse-transcribed, and was subjected to real-time RT-PCR as described previously (21). The mRNA expression of specific genes was quantified using TaqMan gene expression assays (Applied Biosystems, Foster City, CA) as follows: murine *bcl2l1* (assay ID: Mm00437796_m1), murine *fas* (assay ID: Mm01204974_m1), murine *bik* (assay ID: Mm00476123_m1), murine *hrk* (assay ID: Mm01208086_m1), murine *bmf* (assay ID: Mm00506773_m1), and murine *actb* (assay ID: Mm02619580_g1 or Mm00607939_s). The transcript levels are presented as -fold inductions.

siRNA-mediated in Vivo Knockdown—The hepatocyte-specific Bcl-xL-knock-out mice (*bcl-x^{lox/lox}alb-cre*) and the Bcl-xL/Bim/Bid triple knock-out mice (*bim^{-/-}bid^{-/-}bcl-x^{lox/lox}alb-cre*) were injected with 5 mg/kg *in vivo* grade siRNA against *mcl-1* (MSS275671_e0N), which was mixed with InvivoFectamine (Invitrogen), via the tail vein according to the manufacturer's protocol. The mice were sacrificed and examined as indicated by the time courses. The Stealth RNAi negative control with low GC content (Invitrogen) was used as the control.

In Vivo ABT-737 Experiment—ABT-737 was dissolved in a mixture of 30% propylene glycol, 5% Tween 80, and 65% D5W (5% dextrose in water) with pH 4–5. ABT-737 (100 mg/kg) was intraperitoneally administered to the Bim/Bid double knock-

out mice ($bim^{-/-}bid^{-/-}$) or to the Bid-knock-out mice ($bid^{-/-}$). The mice were sacrificed and examined 6 h later.

Statistical Analysis—All of the data are expressed as means \pm S.D. unless otherwise indicated. Statistical analyses were performed using an unpaired Student's *t* test or a one-way analysis of variance unless otherwise indicated. When the analyses of variance were applied, the differences in the mean values among the groups were examined by Scheffe's post hoc correction unless otherwise indicated. $p < 0.05$ was considered statistically significant.

RESULTS

The Disruption of Bim Alleviated Spontaneous Hepatocyte Apoptosis in Hepatocyte-specific Bcl-xL-knock-out Mice—To investigate the involvement of the BH3-only protein Bim in the hepatocyte apoptosis caused by Bcl-xL deficiency, hepatocyte-specific Bcl-xL-knock-out mice ($bcl-x^{fl/fl}alb-cre$) were mated with systemic Bim-knock-out mice ($bim^{-/-}$). Offspring from the mating of $bim^{+/-}bcl-x^{fl/fl}alb-cre$ mice and $bim^{+/-}bcl-x^{fl/fl}$ mice were examined at 6 weeks of age. A Western blot study confirmed the disappearance of both Bcl-xL and Bim protein expression in the liver tissue of the double knock-out mice ($bim^{-/-}bcl-x^{fl/fl}alb-cre$) (Fig. 1A). In agreement with our previous report (7, 17), H&E staining of the liver sections showed an increase in the number of hepatocytes, with chromatin condensation and cytosolic shrinkage in the liver lobules of the Bcl-xL-knock-out mice (Fig. 1B). The staining also showed a significant increase in TUNEL-positive cells and cleaved caspase-3-positive cells in the liver (Fig. 1, B–D). Consistent with these histological observations, the levels of serum caspase-3/7 activity and serum alanine aminotransferase (ALT), which can be used as indicators of hepatocyte apoptosis (22, 23), were significantly higher in the Bcl-xL-knock-out mice than in their wild-type littermates (Fig. 1, E and F). Additionally, cleaved caspase-3 and -7 were detected in the livers of the Bcl-xL-knock-out mice by Western blotting (Fig. 1A). All of these findings indicated spontaneous hepatocyte apoptosis in these mice. Bim-knock-out mice did not show any phenotypes in the liver under physiological conditions (Fig. 1, B–F). Alternatively, the disruption of Bim significantly improved all of the parameters that are indicative of hepatocyte apoptosis in Bcl-xL-knock-out mice, including the TUNEL-positive cell counts, cleaved caspase-3-positive cell counts, serum ALT levels, and serum caspase-3/7 activity (Fig. 1, B–F). These findings clearly demonstrated that Bim was involved in the hepatocyte apoptosis caused by Bcl-xL disruption. It should be noted that the gene and protein expression levels of Bim were not different between the Bcl-xL-knock-out mice and their wild-type littermates (Fig. 1, A and G), indicating that the Bim expression levels observed in the healthy liver could induce hepatocyte apoptosis in the absence of the Bcl-2 family proteins.

The Disruption of Bim Alleviated Spontaneous Hepatocyte Apoptosis in Hepatocyte-specific Mcl-1-knock-out Mice—Of the five members of the anti-apoptotic Bcl-2 family proteins, we previously reported that Mcl-1 and Bcl-xL played a pivotal anti-apoptotic role in maintaining hepatocyte integrity in the healthy liver (13). We thus examined the role of Bim in the hepatocyte apoptosis caused by Mcl-1 deficiency. We gener-

ated Mcl-1/Bim double knock-out mice ($bim^{-/-}mcl-1^{fl/fl}alb-cre$) by mating the hepatocyte-specific Mcl-1-knock-out mice ($mcl-1^{fl/fl}alb-cre$) with the systemic Bim-knock-out mice ($bim^{-/-}$). A Western blot study confirmed the disappearance of both Mcl-1 and Bim protein expression in the liver tissue of the double knock-out mice ($bim^{-/-}mcl-1^{fl/fl}alb-cre$) (Fig. 2A). Consistent with our previous report (13), hepatocyte-specific Mcl-1-knock-out mice showed apoptosis phenotypes very similar to those of the Bcl-xL-knock-out mice, as assessed by TUNEL staining (Fig. 2, B and C), cleaved caspase-3 staining (Fig. 2, B and D), serum caspase-3/7 activity (Fig. 2E), and serum ALT levels (Fig. 2F). In contrast, Mcl-1/Bim double knock-out mice showed significant improvement in these parameters (Fig. 2, B–F), indicating that Bim is also involved in the hepatocyte apoptosis induced by the disruption of Mcl-1.

The Disruption of Bim and Bid Prevented Spontaneous Hepatocyte Apoptosis in Hepatocyte-specific Bcl-xL-knock-out Mice—We previously reported that a small amount of Bid, which is another BH3-only protein, was constitutively active and was involved in the spontaneous hepatocyte apoptosis in Bcl-xL- or Mcl-1-knock-out mice (7, 13). We thus examined whether these BH3-only proteins redundantly or cooperatively promoted hepatocyte apoptosis in the absence of Bcl-xL. To this end, Bim/Bid/Bcl-xL triple knock-out mice ($bim^{-/-}bid^{-/-}bcl-x^{fl/fl}alb-cre$) were generated by mating the Bim/Bcl-xL double knock-out mice ($bim^{-/-}bcl-x^{fl/fl}alb-cre$) with the Bid/Bcl-xL double knock-out mice ($bid^{-/-}bcl-x^{fl/fl}alb-cre$). The offspring from the mating of $bim^{+/-}bid^{-/-}bcl-x^{fl/fl}alb-cre$ mice with $bim^{+/-}bid^{-/-}bcl-x^{fl/fl}$ mice were examined at 6 weeks of age. A Western blot study confirmed that Bcl-xL, Bid, and Bim protein expression disappeared from the liver tissue of the triple knock-out mice ($bim^{-/-}bid^{-/-}bcl-x^{fl/fl}alb-cre$) (Fig. 3A). Liver sections of the Bim/Bid/Bcl-xL triple knock-out mice were histologically normal compared with those of the Bid/Bcl-xL double knock-out mice ($bid^{-/-}bcl-x^{fl/fl}alb-cre$), which still contained some hepatocytes with apoptotic morphologies (Fig. 3B). Both the number of TUNEL-positive cells and the serum caspase-3/7 activity in the triple knock-out mice were significantly lower than those in the Bid/Bcl-xL double knock-out mice and did not differ from their control Bid-knock-out or Bim/Bid double knock-out littermates (Fig. 3, B–D). Moreover, in contrast to the mild elevation of serum ALT levels in the Bid/Bcl-xL double knock-out mice, the levels in the triple knock-out mice were completely normal (Fig. 3E). These findings demonstrated that hepatocyte apoptosis in the absence of Bcl-xL was completely dependent on these two BH3-only proteins.

Bim and Bid Are Essential Regulators for the Promotion of the Intrinsic Pathway of Apoptosis in Hepatocytes in the Absence of Anti-apoptotic Bcl-2 Family Proteins—We then attempted to further examine the involvement of Bim and Bid in hepatocyte apoptosis in the absence of both Bcl-xL and Mcl-1, which are two major anti-apoptotic proteins in the liver. Because, as we reported (13), the hepatocyte-specific Bcl-xL and Mcl-1 double knock-out mice died within 1 day after birth due to impaired liver development, we performed an siRNA-mediated *in vivo* knockdown of *mcl-1* in the Bcl-xL-knock-out mice and in the Bim/Bid/Bcl-xL triple knock-out mice. *mcl-1* siRNA administration efficiently reduced Mcl-1 protein expression in the liver

The Novel Bcl-2 Network in Healthy Liver

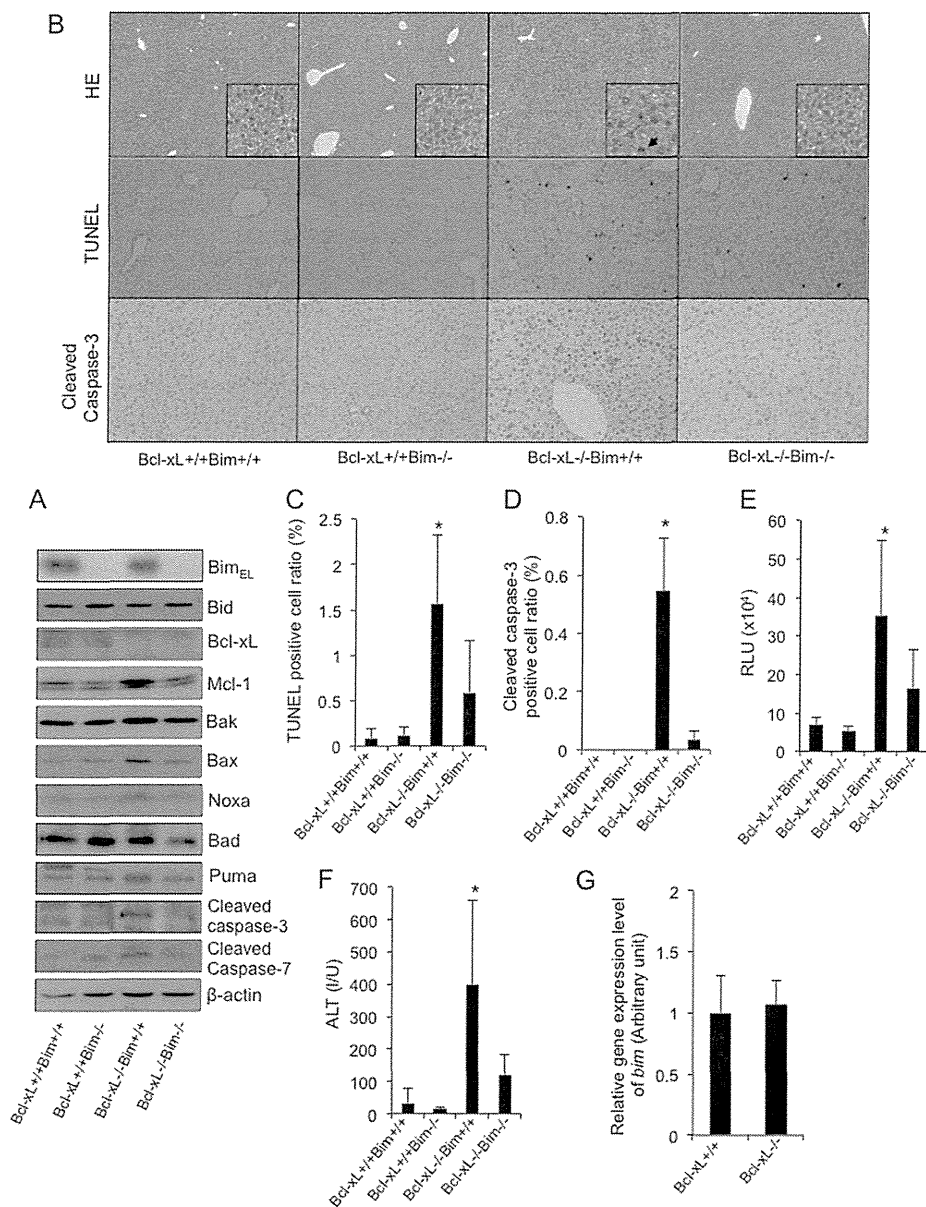


FIGURE 1. The disruption of Bim alleviated spontaneous hepatocyte apoptosis in the absence of Bcl-xL. A–F, the offspring from the mating of *bim*[±]*bcl-xL*^{flax/flax}*alb-cre* mice with *bim*[±]*bcl-xL*^{flax/flax} mice were examined at 6 weeks of age. *Bcl-xL*^{+/+} and *Bcl-xL*^{-/-}, *bcl-xL*^{flax/flax} and *bcl-xL*^{flax/flax}*alb-cre*, respectively. A, Western blot analysis of whole liver lysates for the expression of Bim_{EL}, Bid, Bcl-xL, Mcl-1, Bak, Bax, Noxa, Bad, Puma, cleaved caspase-3, cleaved caspase-7, and β-actin. B, representative images for liver histology stained with hematoxylin-eosin (HE), TUNEL, and cleaved caspase-3 (original magnifications, ×100 (large panels) and ×400 (insets)); black arrows indicate apoptotic bodies. C, TUNEL-positive cell ratio; n = 8 mice/group; *p < 0.05 versus all. D, cleaved caspase-3-positive cell ratio; n = 3 mice/group; *p < 0.05 versus all. E, serum caspase-3/7 activity; n = 11 mice/group; *p < 0.05 versus all. F, serum ALT levels; n = 13 mice/group; *p < 0.05 versus all. G, offspring from the mating of *bcl-xL*^{flax/flax}*alb-cre* mice with *bcl-xL*^{flax/flax} mice were examined at 6 weeks of age. *Bcl-xL*^{+/+} and *Bcl-xL*^{-/-}, *bcl-xL*^{flax/flax} and *bcl-xL*^{flax/flax}*alb-cre*, respectively. *bim* mRNA levels in the whole liver tissue were determined by real-time RT-PCR; n = 6 mice/group. Error bars, S.D. RLU, relative light units; IU, international units.

tissue of both mice (Fig. 4A), but it caused severe liver injury only in the *Bcl-xL*-knock-out mice (Fig. 4B) when assessed by the H&E staining of liver sections. Notably, *mcl-1* siRNA administration caused massive hepatocyte apoptosis in the *Bcl-xL*-knock-out mice, but this apoptosis was weakened in the *Bim*/*Bid*/*Bcl-xL* triple knock-out mice, as evidenced by the TUNEL staining of the liver sections, serum caspase-3/7 activity, and serum ALT levels (Fig. 4, C–E). In agreement with these findings, *mcl-1* siRNA treatment impaired the liver function of the *Bcl-xL*-knock-out mice, as evidenced by an increase in the

serum bilirubin levels, but not the liver function of the triple knock-out mice (Fig. 4F). These findings demonstrated that the massive hepatocyte apoptosis and liver failure caused by decreases in these anti-apoptotic *Bcl-2* family proteins were dependent on *Bid* and *Bim*.

The Presence of Bim- and Bid-induced Constant BH3 Stress in the Healthy Liver Causes Hepatotoxicity with the Use of Anti-cancer Agents That Target the Anti-apoptotic Bcl-2 Family Proteins—Recent advances in cancer therapy have enabled the selective targeting of some anti-apoptotic *Bcl-2* family proteins,

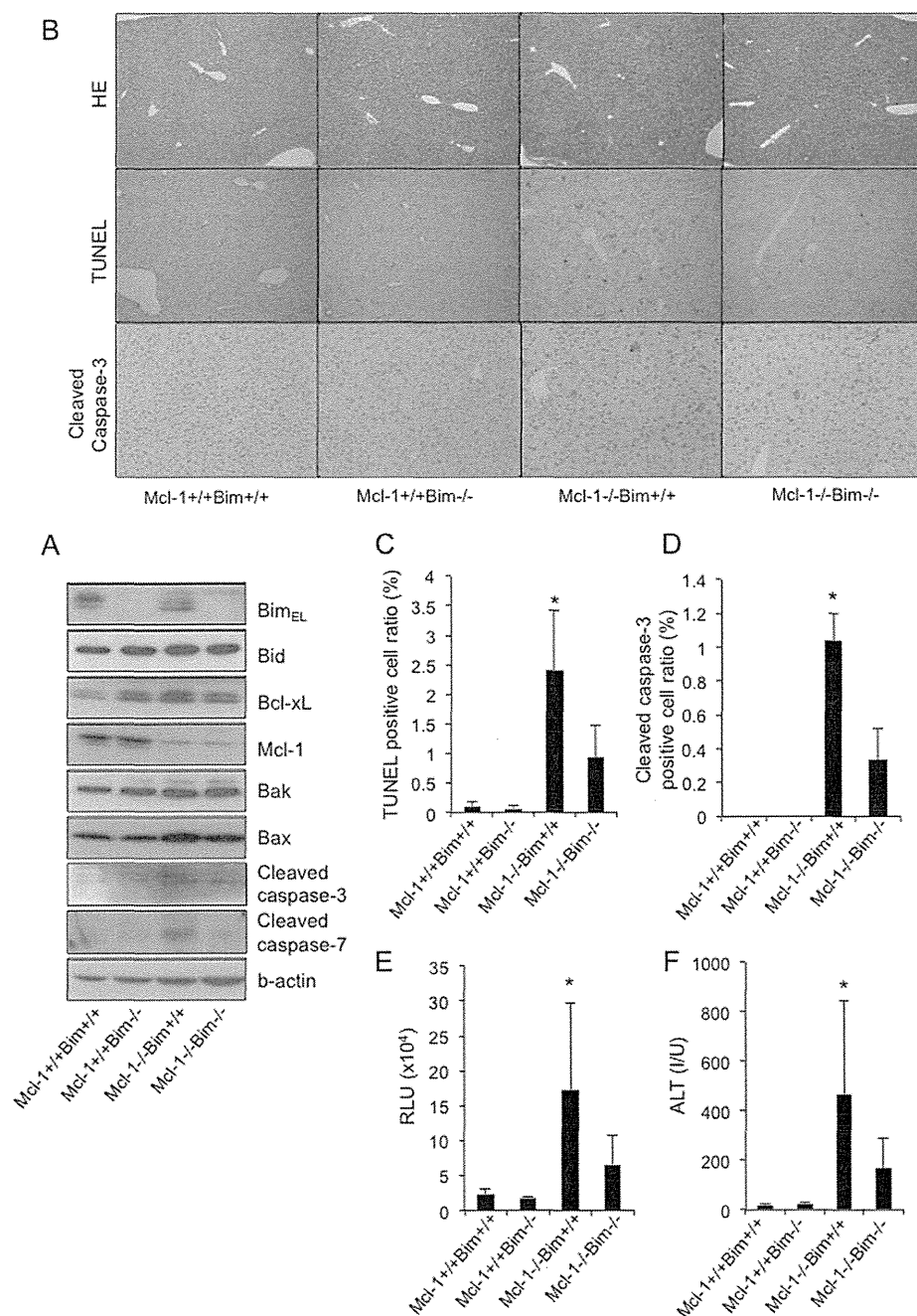


FIGURE 2. The disruption of Bim alleviated spontaneous hepatocyte apoptosis in the absence of Mcl-1. The offspring from the mating of *bim*^{+/-}*mcl-1*^{fllox/fllox}*alb-cre* mice with *bim*^{+/-}*mcl-1*^{fllox/fllox} mice were examined at 6 weeks of age. *Mcl-1*^{+/+} and *Mcl-1*^{-/-}, *mcl-1*^{fllox/fllox} and *mcl-1*^{fllox/fllox}*alb-cre*, respectively. *A*, Western blot analysis of whole liver lysates for the expression of Bim_{EL}, Bid, Bcl-xL, Mcl-1, Bak, Bax, cleaved caspase-3, cleaved caspase-7, and β-actin. *B*, representative images for liver histology stained with hematoxylin-eosin (HE), TUNEL, and cleaved caspase-3 (original magnification, ×100). *C*, TUNEL-positive cell ratio; *n* = 3–6 mice/group; *, *p* < 0.05 versus all. *D*, cleaved caspase-3-positive cell ratio; *n* = 3 mice/group; *, *p* < 0.05 versus all. *E*, serum caspase-3/7 activity; *n* = 9–15 mice/group; *, *p* < 0.05 versus all. *F*, serum ALT levels; *n* = 9–15 mice/group; *, *p* < 0.05 versus all. Error bars, S.D. RLU, relative light units; I/U, international units.

which are often dysregulated in malignant cells. ABT-737, which is a BH3 mimetic, could inhibit Bcl-xL, Bcl-2, and Bcl-w, and it has induced the regression of solid tumors (23). We previously reported that high dose ABT-737 administration caused hepatocyte apoptosis even in a normal liver, which was partly due to constitutive Bid-mediated BH3 stress (7). This finding led us to investigate the involvement of Bim and Bid in this ABT-737-mediated hepatotoxicity. Bim/Bid double

knock-out mice (*bim*^{-/-}*bid*^{-/-}) were generated by mating Bim knock-out mice (*bim*^{-/-}) with Bid knock-out mice (*bid*^{-/-}), and the offspring were then treated with this drug. Western blot analysis confirmed the efficient deletion of Bim and Bid from the liver tissue of the double knock-out mice (Fig. 5A). Upon ABT-737 treatment, the Bim/Bid double knock-out mice showed complete prevention of ABT-737-induced hepatocyte apoptosis and hepatotoxicity (Fig. 5, B–F), in sharp con-

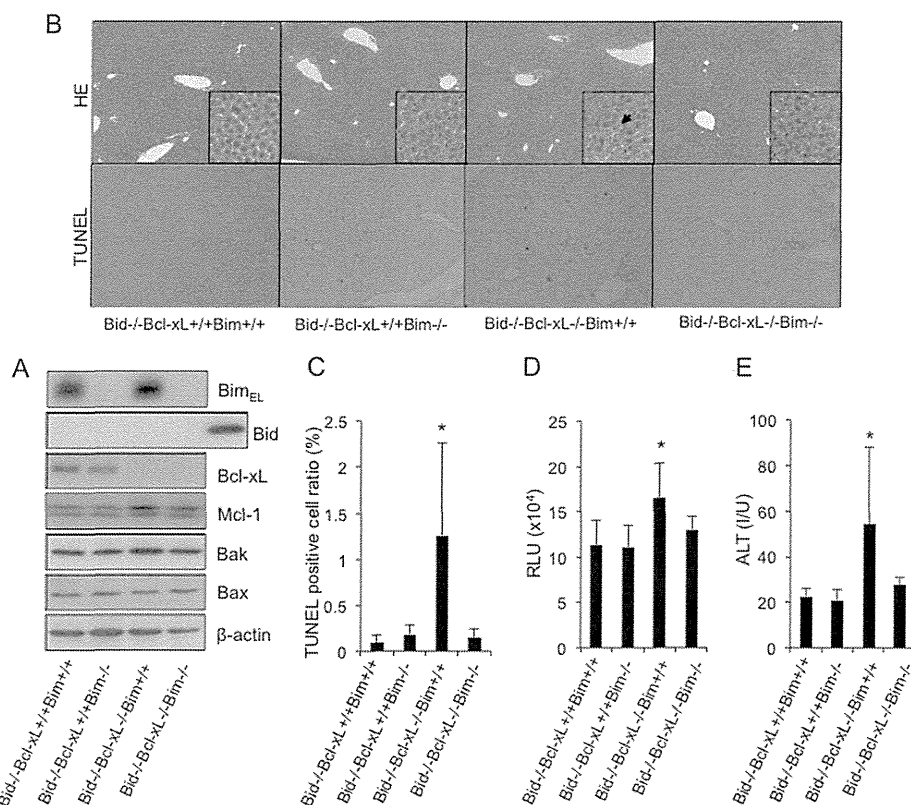


FIGURE 3. The disruption of Bim and Bid prevented spontaneous hepatocyte apoptosis in the absence of Bcl-xL. The offspring from the mating of *bim*^{+/-}*bid*^{-/-}*bcl-x*^{flx/flx}*alb-cre* mice with *bim*^{+/-}*bid*^{-/-}*bcl-x*^{flx/flx} mice were examined at 6 weeks of age. *Bcl-xL*^{+/+} and *Bcl-xL*^{-/-}, *bcl-x*^{flx/flx} and *bcl-x*^{flx/flx}*alb-cre*, respectively. *A*, Western blot analysis of whole liver lysates for the expression of Bim_{EL}, Bid, Bcl-xL, Mcl-1, Bak, Bax, and β-actin. *B*, representative images of liver histology stained with hematoxylin-eosin (HE) and TUNEL (original magnifications, ×100 (large panels) and ×400 (insets)). Black arrows indicate apoptotic bodies. *C*, TUNEL-positive cell ratio; more than 5 mice/group; *, *p* < 0.05 versus all. *D*, serum caspase-3/7 activity; more than 6 mice/group; *, *p* < 0.05 versus all. *E*, serum ALT levels; more than 6 mice/group; *, *p* < 0.05 versus all. Error bars, S.D. RLU, relative light units; /U, international units.

trast to their Bid-knock-out littermates, which still showed moderate hepatocyte apoptosis (Fig. 5, C–E) and increased serum ALT levels (Fig. 5F). These findings suggested that Bim- and Bid-mediated constant BH3 stress evoked hepatotoxicity by promoting the intrinsic pathway of apoptosis with the use of the inhibitors of the Bcl-2 family.

DISCUSSION

At least eight BH3-only proteins are known, and five have been reported to exist in hepatocytes: Bid, Bim, Noxa, Puma, and Bad (22). We also confirmed these five proteins in the liver tissue of our mice (Fig. 1A), and we detected at least the mRNA expression of three other genes (supplemental Fig. 1). These proteins are considered to function as pro-apoptotic sensors upon activation by a variety of apoptotic stimuli, thereby promoting an intrinsic pathway of apoptosis in a manner that is dependent on the presence of Bak and Bax. In previous studies, bile acids or death receptor stimuli activated Bid and induced liver injury, which was alleviated by Bid disruption (12, 22). Bim activation was involved in hepatocyte lipoapoptosis, which is a critical feature of non-alcoholic steatohepatitis, and in reactive oxygen species-induced hepatocyte apoptosis (10, 11, 14). Additionally, a recent *in vivo* study revealed that the activation of Bid and Bim played a central pro-apoptotic role in fatal TNF-α-induced hepatitis (24). Taken together, these findings indicated the importance of these two BH3-only proteins in the

pathogenesis of various liver diseases (12, 24, 25). Conversely, the systemic knock-out of Bid or Bim in mice did not result in any liver abnormalities under normal conditions; therefore, there has not been much interest in studying their physiological involvement in the healthy liver (12, 26). However, our present study showed that spontaneous hepatocyte apoptosis in the absence of Bcl-xL was alleviated by the deletion of either Bim or Bid, and it was diminished by the deletion of both. These results indicated that these BH3-only proteins are functionally active even in the healthy liver, but they are fully restrained by the anti-apoptotic Bcl-2 family proteins in the physiological state.

What type of stimuli constitutively activate these BH3-only proteins remains unknown. The liver is a specific organ that can be continuously exposed to a variety of stimuli, such as bile acids and enteric endotoxin, as well as interactions with immune cells. These stimuli might cause constitutive BH3-only stress through the activation of death receptors, such as Fas, tumor necrosis factor (TNF), and TNF-related apoptosis-inducing ligand (TRAIL) receptors. To explore the involvement of Fas signaling in generating this BH3-only stress, we studied the effect of *fas* inhibition in the hepatocyte apoptosis induced by the genetic disruption of Bcl-xL or ABT-737 administration. siRNA-mediated *in vivo* knockdown of *fas* did not alleviate their hepatocyte apoptosis (supplemental Fig. 2, B and D), suggesting that Fas signaling may not be the origin of this BH3-only

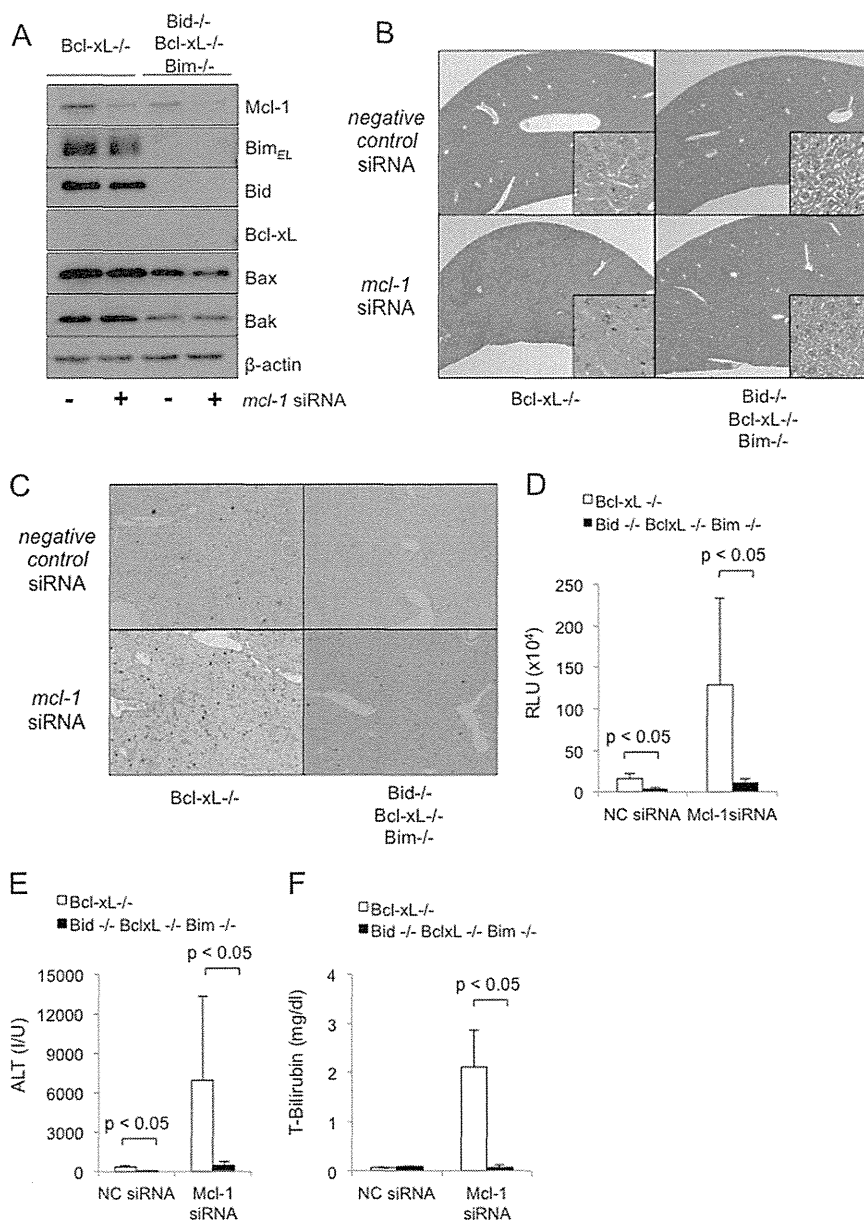


FIGURE 4. Bim and Bid are essential regulators involved in the intrinsic pathway of apoptosis in hepatocytes in the absence of anti-apoptotic Bcl-2 family proteins. *bcl-x^{fllox/fllox} alb-cre* mice and *bim^{-/-} bid^{-/-} bcl-x^{fllox/fllox} alb-cre* mice were injected with *mcl-1* or with negative control siRNA via the tail vein and were sacrificed 24 h (A and C–F) or 48 h (B) later. *Bcl-xL^{+/+}* and *Bcl-xL^{-/-}*, *bcl-x^{fllox/fllox}* and *bcl-x^{fllox/fllox} alb-cre*, respectively. NC, negative control. A, Western blot analysis of whole liver lysates for the expression of Bim_{EL}, Bid, Bcl-xL, Mcl-1, Bak, Bax, and β-actin. B, representative images of liver histology stained with hematoxylin-eosin (original magnifications, ×100 (large panels) and ×400 (insets)). C, representative images of liver histology stained with TUNEL (original magnification, ×100). D, serum caspase-3/7 activity; n = 3–4 mice/group. E, serum ALT levels; n = 4 mice/group; data are presented as means ± S.E. (error bars). F, serum T-bilirubin levels; n = 4 mice/group. RLU, relative light units; IU, international units.

stress. However, it should be noted here that siRNA administration only decreased *fas* mRNA levels to around half (supplemental Fig. 2, A and C). Therefore, genetic study is still necessary to clarify its involvement. In order to examine the involvement of T and B cells, which comprise about 50% of intrahepatic resident immune cells (27), in producing the BH3-only stress in the healthy liver, we crossed hepatocyte-specific Mcl-1 knock-out mice with homozygous SCID mutant mice, which are characterized by an absence of functional T cells and B cells (28). The spontaneous hepatocyte apoptosis of the Mcl-1 knock-out mice was unchanged even in the homozygous SCID

mutant background, monitored by serum ALT levels and serum caspase-3/7 activity (supplemental Fig. 3, A–D). These data indicate that these immune cells are not the major source of the BH3-only stress in the liver under physiological conditions. Therefore, further study is required to identify the main source of constitutive BH3-only stress in the healthy liver. We previously reported that Mcl-1 and Bcl-xL individually worked as apoptotic antagonists in differentiated hepatocytes (13). However, the hepatocyte-specific deletion of both led to early postnatal death due to the failure of hepatocyte development in the fetal liver (13), thus hampering the clarification of their

The Novel Bcl-2 Network in Healthy Liver

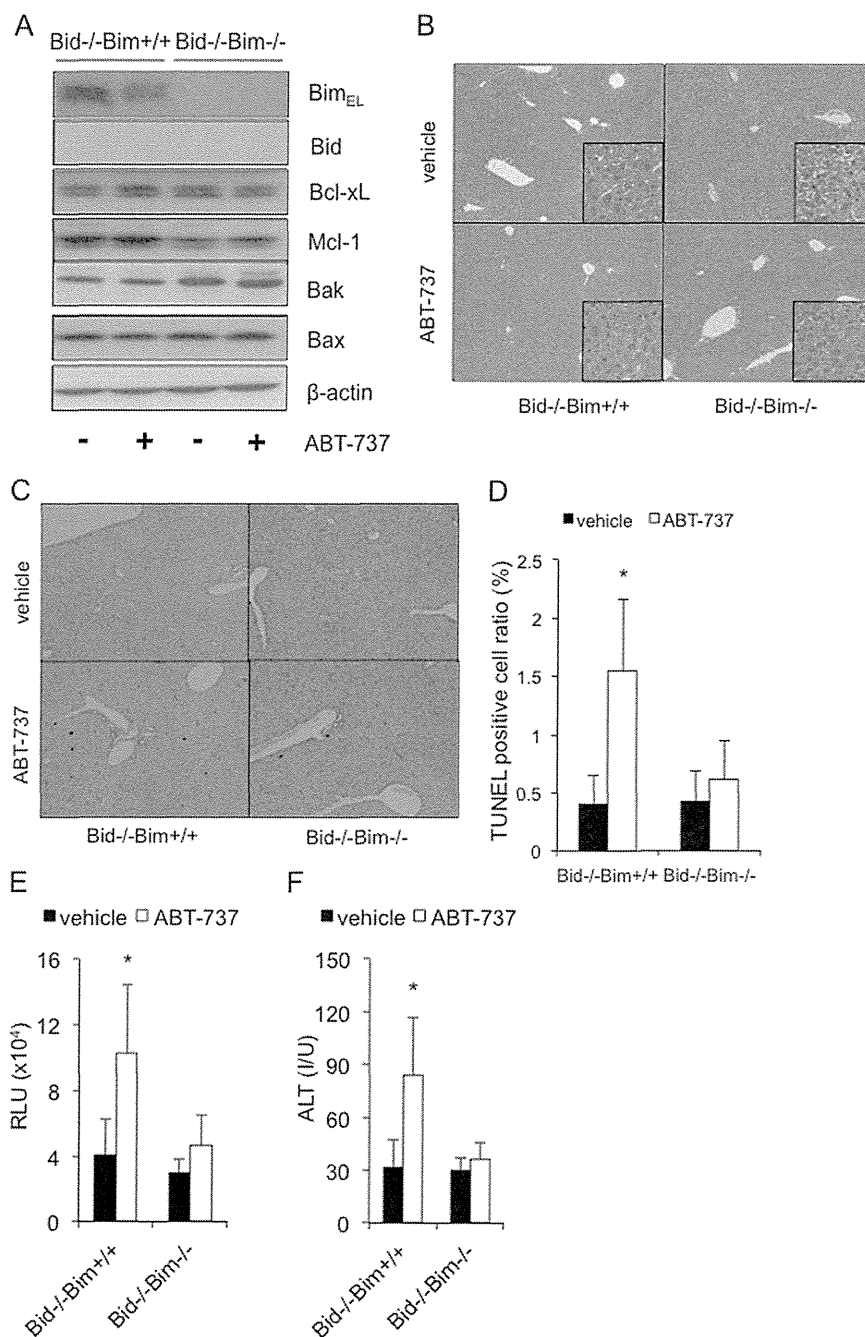


FIGURE 5. The presence of Bim- and Bid-induced constant BH3 stress in the healthy liver causes hepatotoxicity with the use of anti-cancer agents that target anti-apoptotic Bcl-2 family proteins. The offspring from *bim*^{+/+}*bid*^{-/-} mating pairs were given an intraperitoneal injection of ABT-737 (100 mg/kg) or vehicle and were examined after 6 h. *A*, Western blot analysis of whole liver lysates for the expression of Bim_{EL}, Bid, Bcl-xL, Mcl-1, Bak, Bax, and β-actin. *B* and *C*, representative images of liver histology stained with hematoxylin-eosin and TUNEL (original magnifications, ×100 (large panels) and ×400 (insets)). *D*, TUNEL-positive cell ratio; *n* = 5–6 mice/group; *, *p* < 0.05 versus all. *E*, serum caspase-3/7 activity; more than 5 mice/group; *, *p* < 0.05 versus all. *F*, serum ALT levels; more than 5 mice/group; *, *p* < 0.05 versus all. Error bars, S.D. RLU, relative light units; IU, international units.

cooperative involvement in the adult liver. In the present study, the combination of genetically engineered mice and *in vivo* siRNA technology enabled the investigation of their cooperative roles for the first time, and we found that the inhibition of Mcl-1 caused sublethal liver injury with massive hepatocyte apoptosis in Bcl-xL-knock-out mice. Meanwhile, we also found that sublethal apoptosis was prevented in a Bim/Bid double knock-out background, suggesting that, of the BH3-only

proteins, Bim and Bid are important for activating the intrinsic pathway of hepatocyte apoptosis in the absence of anti-apoptotic Bcl-2 family proteins. It would also be interesting to determine whether other anti-apoptotic Bcl-2 family proteins or BH3-only proteins are involved in this healthy Bcl-2 rheostasis.

The anti-apoptotic Bcl-2 family proteins are often dysregulated in a variety of malignancies, and they have been recog-

nized as important oncogenes (29). ABT-737, which was recently developed to inhibit the Bcl-xL, Bcl-w, and Bcl-2 proteins, displays anti-tumor activity against lymphoid malignancies and small-cell lung carcinoma (23). These drugs were considered to selectively target tumor cells because malignant cells receive many genotoxic and environmental stress-induced BH3-only signals, so these cells are thus dependent on the anti-apoptotic Bcl-2 family members for their survival. However, we previously reported that the high-dose administration of ABT-737 (100 mg/kg) elicited hepatotoxicity via Bak/Bax-dependent apoptosis in normal hepatocytes (7), suggesting that dependence on the anti-apoptotic Bcl-2 family proteins is not a specific feature of tumor cells but is the case in healthy liver cells. In the present study, we demonstrated that the disruption of Bim and Bid completely prevented hepatocyte apoptosis and hepatotoxicity induced by high dose ABT-737 (100 mg/kg), suggesting that these proteins are responsible for this hepatotoxicity. Meanwhile, although 25 mg/kg ABT-737, which is relatively close to the clinical dose, caused moderate hepatocyte apoptosis, this apoptosis was completely blocked by Bid inhibition (supplemental Fig. 4). Therefore, it is unclear whether both Bid and Bim are truly involved in hepatotoxicity when using ABT-737 at clinically relevant doses.

This study demonstrated that Bim was also involved in the hepatocyte apoptosis caused by Mcl-1 deficiency in addition to Bid, which was noted in our previous report (13). Several previous human studies have reported that Mcl-1 proteins were down-regulated in the liver tissues of non-alcoholic steatohepatitis and primary biliary cirrhosis patients (30, 31), and experimental studies have demonstrated that Mcl-1 down-regulation by saturated fatty acids caused hepatocyte lipoapoptosis, which plays an important role in the development of fatty liver disease (32, 33). Taken together with our findings, these reports suggest the possibility that Bim- and Bid-mediated constant BH3 stresses might constitute therapeutic targets of the hepatotoxicity observed in these human liver diseases.

In conclusion, we have demonstrated that the novel rheostatic balance between the pro-apoptotic BH3-only proteins Bim and Bid and the anti-apoptotic Bcl-2 family proteins Bcl-xL and Mcl-1 regulates hepatocyte life and death in the physiological state. Our present study sheds new light on the dynamic and well orchestrated Bcl-2 networks in the healthy liver.

Acknowledgments—We thank Lothar Hennighausen (National Institutes of Health) and Dr. You-Wen He (Duke University) for providing the floxed *bcl-x* mice and floxed *mcl-1* mice, respectively. We also thank Abbott Laboratories for providing ABT-737.

REFERENCES

1. Youle, R. J., and Strasser, A. (2008) The BCL-2 protein family. Opposing activities that mediate cell death. *Nat. Rev. Mol. Cell Biol.* **9**, 47–59
2. Chipuk, J. E., and Green, D. R. (2008) How do BCL-2 proteins induce mitochondrial outer membrane permeabilization? *Trends Cell Biol.* **18**, 157–164
3. Adams, J. M., and Cory, S. (2007) Bcl-2-regulated apoptosis. Mechanism and therapeutic potential. *Curr. Opin. Immunol.* **19**, 488–496
4. Kim, H., Rafiuddin-Shah, M., Tu, H. C., Jeffers, J. R., Zambetti, G. P., Hsieh, J. J., and Cheng, E. H. (2006) Hierarchical regulation of mitochondrion-dependent apoptosis by BCL-2 subfamilies. *Nat. Cell Biol.* **8**, 1348–1358
5. Willis, S. N., Fletcher, J. I., Kaufmann, T., van Delft, M. F., Chen, L., Czabotar, P. E., Ierino, H., Lee, E. F., Fairlie, W. D., Bouillet, P., Strasser, A., Kluck, R. M., Adams, J. M., and Huang, D. C. (2007) Apoptosis initiated when BH3 ligands engage multiple Bcl-2 homologs, not Bax or Bak. *Science* **315**, 856–859
6. Korsmeyer, S. J., Shutter, J. R., Veis, D. J., Merry, D. E., and Oltvai, Z. N. (1993) Bcl-2/Bax. A rheostat that regulates an anti-oxidant pathway and cell death. *Semin. Cancer Biol.* **4**, 327–332
7. Hikita, H., Takehara, T., Kodama, T., Shimizu, S., Hosui, A., Miyagi, T., Tatsumi, T., Ishida, H., Ohkawa, K., Li, W., Kanto, T., Hiramatsu, N., Hennighausen, L., Yin, X. M., and Hayashi, N. (2009) BH3-only protein bid participates in the Bcl-2 network in healthy liver cells. *Hepatology* **50**, 1972–1980
8. Giam, M., Huang, D. C., and Bouillet, P. (2008) BH3-only proteins and their roles in programmed cell death. *Oncogene* **27**, Suppl. 1, S128–S136
9. Lomonosova, E., and Chinnadurai, G. (2008) *Oncogene* **27**, Suppl. 1, S2–S19
10. Barreiro, F. J., Kobayashi, S., Bronk, S. F., Werneburg, N. W., Malhi, H., and Gores, G. J. (2007) Transcriptional regulation of Bim by FoxO3A mediates hepatocyte lipoapoptosis. *J. Biol. Chem.* **282**, 27141–27154
11. Ishihara, Y., Takeuchi, K., Ito, F., and Shimamoto, N. (2011) Dual regulation of hepatocyte apoptosis by reactive oxygen species. Increases in transcriptional expression and decreases in proteasomal degradation of BimEL. *J. Cell Physiol.* **226**, 1007–1016
12. Yin, X. M., Wang, K., Gross, A., Zhao, Y., Zinkel, S., Klocke, B., Roth, K. A., and Korsmeyer, S. J. (1999) Bid-deficient mice are resistant to Fas-induced hepatocellular apoptosis. *Nature* **400**, 886–891
13. Hikita, H., Takehara, T., Shimizu, S., Kodama, T., Li, W., Miyagi, T., Hosui, A., Ishida, H., Ohkawa, K., Kanto, T., Hiramatsu, N., Yin, X. M., Hennighausen, L., Tatsumi, T., and Hayashi, N. (2009) Mcl-1 and Bcl-xL cooperatively maintain integrity of hepatocytes in developing and adult murine liver. *Hepatology* **50**, 1217–1226
14. Ishihara, Y., Ito, F., and Shimamoto, N. (2011) Increased expression of c-Fos by extracellular signal-regulated kinase activation under sustained oxidative stress elicits BimEL upregulation and hepatocyte apoptosis. *FEBS J.* **278**, 1873–1881
15. Malhi, H., Bronk, S. F., Werneburg, N. W., and Gores, G. J. (2006) Free fatty acids induce JNK-dependent hepatocyte lipoapoptosis. *J. Biol. Chem.* **281**, 12093–12101
16. Dzhagalov, I., St John, A., and He, Y. W. (2007) The antiapoptotic protein Mcl-1 is essential for the survival of neutrophils but not macrophages. *Blood* **109**, 1620–1626
17. Takehara, T., Tatsumi, T., Suzuki, T., Rucker, E. B., 3rd, Hennighausen, L., Jinushi, M., Miyagi, T., Kanazawa, Y., and Hayashi, N. (2004) Hepatocyte-specific disruption of Bcl-xL leads to continuous hepatocyte apoptosis and liver fibrotic responses. *Gastroenterology* **127**, 1189–1197
18. Wagner, K. U., Claudio, E., Rucker, E. B., 3rd, Riedlinger, G., Broussard, C., Schwartzberg, P. L., Siebenlist, U., and Hennighausen, L. (2000) Conditional deletion of the Bcl-x gene from erythroid cells results in hemolytic anemia and profound splenomegaly. *Development* **127**, 4949–4958
19. Maruyama, C., Suemizu, H., Tamamushi, S., Kimoto, S., Tamaoki, N., and Ohnishi, Y. (2002) Genotyping the mouse severe combined immunodeficiency mutation using the polymerase chain reaction with confronting two-pair primers (PCR-CTPP). *Exp. Anim.* **51**, 391–393
20. Kodama, T., Takehara, T., Hikita, H., Shimizu, S., Shigekawa, M., Tsunematsu, H., Li, W., Miyagi, T., Hosui, A., Tatsumi, T., Ishida, H., Kanto, T., Hiramatsu, N., Kubota, S., Takigawa, M., Tomimaru, Y., Tomokuni, A., Nagano, H., Doki, Y., Mori, M., and Hayashi, N. (2011) Increases in p53 expression induce CTGF synthesis by mouse and human hepatocytes and result in liver fibrosis in mice. *J. Clin. Invest.* **121**, 3343–3356
21. Kodama, T., Takehara, T., Hikita, H., Shimizu, S., Li, W., Miyagi, T., Hosui, A., Tatsumi, T., Ishida, H., Tadokoro, S., Ido, A., Tsubouchi, H., and Hayashi, N. (2010) Thrombocytopenia exacerbates cholestasis-induced liver fibrosis in mice. *Gastroenterology* **138**, 2487–2498, 2498.e2481–2487
22. Baskin-Bey, E. S., and Gores, G. J. (2005) Death by association. BH3 domain-only proteins and liver injury. *Am. J. Physiol. Gastrointest. Liver Physiol.* **289**, G987–G990
23. Oltersdorf, T., Elmore, S. W., Shoemaker, A. R., Armstrong, R. C., Augeri,

The Novel Bcl-2 Network in Healthy Liver

- D. J., Belli, B. A., Bruncko, M., Deckwerth, T. L., Dinges, J., Hajduk, P. J., Joseph, M. K., Kitada, S., Korsmeyer, S. J., Kunzer, A. R., Letai, A., Li, C., Mitten, M. J., Nettesheim, D. G., Ng, S., Nimmer, P. M., O'Connor, J. M., Oleksijew, A., Petros, A. M., Reed, J. C., Shen, W., Tahir, S. K., Thompson, C. B., Tomaselli, K. J., Wang, B., Wendt, M. D., Zhang, H., Fesik, S. W., and Rosenberg, S. H. (2005) An inhibitor of Bcl-2 family proteins induces regression of solid tumours. *Nature* **435**, 677–681
24. Kaufmann, T., Jost, P. J., Pellegrini, M., Puthalakath, H., Gugasyan, R., Gerondakis, S., Cretney, E., Smyth, M. J., Silke, J., Hakem, R., Bouillet, P., Mak, T. W., Dixit, V. M., and Strasser, A. (2009) Fatal hepatitis mediated by tumor necrosis factor TNF α requires caspase-8 and involves the BH3-only proteins Bid and Bim. *Immunity* **30**, 56–66
25. Higuchi, H., Miyoshi, H., Bronk, S. F., Zhang, H., Dean, N., and Gores, G. J. (2001) Bid antisense attenuates bile acid-induced apoptosis and cholestatic liver injury. *J. Pharmacol. Exp. Ther.* **299**, 866–873
26. Bouillet, P., Metcalf, D., Huang, D. C., Tarlinton, D. M., Kay, T. W., Köntgen, F., Adams, J. M., and Strasser, A. (1999) Proapoptotic Bcl-2 relative Bim required for certain apoptotic responses, leukocyte homeostasis, and to preclude autoimmunity. *Science* **286**, 1735–1738
27. Blom, K. G., Qazi, M. R., Matos, J. B., Nelson, B. D., DePierre, J. W., and Abedi-Valugerdi, M. (2009) Isolation of murine intrahepatic immune cells employing a modified procedure for mechanical disruption and functional characterization of the B, T, and natural killer T cells obtained. *Clin. Exp. Immunol.* **155**, 320–329
28. Shultz, L. D., Schweitzer, P. A., Christianson, S. W., Gott, B., Schweitzer, I. B., Tennent, B., McKenna, S., Mobraaten, L., Rajan, T. V., and Greiner, D. L. (1995) Multiple defects in innate and adaptive immunologic function in NOD/LtSz-scid mice. *J. Immunol.* **154**, 180–191
29. Kirkin, V., Joos, S., and Zörnig, M. (2004) The role of Bcl-2 family members in tumorigenesis. *Biochim. Biophys. Acta* **1644**, 229–249
30. García-Monzon, C., Lo Iacono, O., Mayoral, R., González-Rodríguez, A., Miquilena-Colina, M. E., Lozano-Rodríguez, T., García-Pozo, L., Vargas-Castrillón, J., Casado, M., Boscá, L., Valverde, A. M., and Martín-Sanz, P. (2011) Hepatic insulin resistance is associated with increased apoptosis and fibrogenesis in nonalcoholic steatohepatitis and chronic hepatitis C. *J. Hepatol.* **54**, 142–152
31. Iwata, M., Harada, K., Kono, N., Kaneko, S., Kobayashi, K., and Nakanuma, Y. (2000) Expression of Bcl-2 familial proteins is reduced in small bile duct lesions of primary biliary cirrhosis. *Hum. Pathol.* **31**, 179–184
32. Ibrahim, S. H., Kohli, R., and Gores, G. J. (2011) Mechanisms of lipotoxicity in NAFLD and clinical implications. *J. Pediatr. Gastroenterol. Nutr.* **53**, 131–140
33. Masuoka, H. C., Mott, J., Bronk, S. F., Werneburg, N. W., Akazawa, Y., Kaufmann, S. H., and Gores, G. J. (2009) Mcl-1 degradation during hepatocyte lipapoptosis. *J. Biol. Chem.* **284**, 30039–30048